Preprocedural CT Evaluation of Transcatheter Aortic Valve Replacement: What the Radiologist Needs to Know[1]

Rodrigo A. Salgado, MD
Jonathon A. Leipsic, MD
Bharati Shivalkar, MD, PhD
Lenz Ardies, MD
Paul L. Van Herck, MD, PhD
Bart J. Op de Beeck, MD
Christiaan Vrints, MD, PhD
Inez Rodrigus, MD, PhD
Paul M. Parizel, MD, PhD
Johan Bosmans, MD, PhD

Aortic valve stenosis is the most common valvular heart disease in the Western world. When symptomatic, aortic valve stenosis is a debilitating disease with a dismal short-term prognosis, invariably leading to heart failure and death. Elective surgical valve replacement has traditionally been considered the standard of care for symptomatic aortic valve stenosis. However, several studies have identified various subgroups of patients with a significantly elevated risk for surgery-related complications and death. Thus, not every patient is a suitable candidate for surgery. Recent developments in transcatheter-based therapies have provided an alternative therapeutic strategy for the nonsurgical patient population known as transcatheter aortic valve replacement (TAVR) (also called transcatheter aortic valve implantation or percutaneous aortic valve replacement). In TAVR, the native aortic valve is replaced with a bioprosthetic valve via a nonsurgical endovascular, transaortic, or transapical pathway. Nevertheless, several anatomic and technical criteria must be met to safeguard patient eligibility and procedural success. Therefore, noninvasive imaging plays a crucial role in both patient selection and subsequent matching to a specific transcatheter valve size in an effort to ensure accurate prosthesis deployment and minimize peri- and postprocedural complications. The authors review the relevant anatomy of the aortic root, emphasizing the implications of anatomic pitfalls for correct reporting of imaging-derived measurements and important differences between findings obtained with different imaging modalities. They also discuss the evolving role of computed tomography and the role of the radiologist in patient triage in light of current viewpoints regarding patient selection, device size selection, and the preprocedural evaluation of possible access routes. *Online supplemental material is available for this article.*

Abbreviations: ECG = electrocardiography, LVOT = left ventricular outflow tract, PAR = paravalvular aortic regurgitation, SFAR = ratio of sheath size to femoral artery size, TAVR = transcatheter aortic valve replacement, TEE = transesophageal echocardiography, 3D = three-dimensional, TTE = transthoracic echocardiography, 2D = two-dimensional

RadioGraphics 2014; 34:1491–1514

Published online 10.1148/rg.346125076

Content Codes: CA CH CT

[1]From the Departments of Radiology (R.A.S., L.A., B.J.O.d.B., P.M.P.), Cardiology (B.S., P.L.V.H., C.V., J.B.), and Cardiothoracic Surgery (I.R.), Antwerp University Hospital, Wilrijkstraat 10, 2650 Edegem-Antwerp, Belgium; and Department of Radiology, Department of Medical Imaging, St Paul's Hospital, University of British Columbia, Vancouver, BC, Canada (J.A.L.). Recipient of a Cum Laude award for an education exhibit at the 2011 RSNA Annual Meeting. Received April 12, 2012; revision requested May 9; final revision received May 3, 2013; accepted May 28. For this journal-based SA-CME activity, the author J.A.L. has provided disclosures (see p 1510); all other authors, the editor, and the reviewers have disclosed no relevant relationships. **Address correspondence to** R.A.S. (e-mail: *rodrigo.salgado@uza.be*).

See discussion on this article by Martínez-Jiménez (pp 1514–1516).

See also the article by Salgado et al (pp 1517–1536) in this issue.

Scan this code for access to supplemental material on our website.

TEACHING POINTS

See last page

SA-CME LEARNING OBJECTIVES

After completing this journal-based SA-CME activity, participants will be able to:

- Describe the complex anatomy of the aortic root and its different components, as well as the implications for correct measurement and reporting of imaging findings.
- Discuss the various viewpoints regarding sizing of the aortic annulus using noninvasive imaging techniques, the specific problems associated with 2D versus 3D imaging modalities, and potential solutions.
- List other important preoperative parameters and predictors of peri- and postprocedural complications.

See www.rsna.org/education/search/RG.

Introduction

Severe aortic valve stenosis is the most common valvular heart disease in Western nations, mostly secondary to the aging process and increased life expectancy. In recent years, new therapeutic options have emerged with the introduction of transcatheter valves for specific subpopulations. All preoperative information required

for patient selection and correct matching to a specific transcatheter valve size is obtained almost exclusively with noninvasive imaging methods. In this article, we discuss the current state of treatment using this new technique, with emphasis on the relevant anatomy of the aortic root and the role of multidetector computed tomography (CT) in patient selection, device size selection, and the preprocedural evaluation of possible access routes.

Definition and Clinical Consequences of Aortic Valve Stenosis

Aortic valve stenosis is defined as an obstruction of the left ventricular outflow tract (LVOT) at or near the level of the aortic valve, with an aortic stenosis jet velocity of over 4 m/sec, a mean gradient of over 40–50 mm Hg, and an aortic valve area of less than 1.0 cm^2 (1). Critical aortic valve stenosis is reached when the valve area is less than 0.6 cm^2. Although aortic valve stenosis can be sub- or supravalvular, the valvular form is most frequently encountered in adults. Its overall prevalence is estimated to be 5%, mostly affecting the elderly population, with 2%–3% of individuals over 75 years of age having severe aortic valve stenosis (2). Aortic valve stenosis is a progressive disease that evolves from a nonsymptomatic valve with thickened and calcified leaflets but without hemodynamic repercussions into an increasingly degenerative valve with extensive calcified and immobile leaflets. As the valve stenosis worsens, symptoms progress from mild to severe, with increasing fatigue and shortness of breath being common complaints and with the condition invariably leading to heart failure. The final symptomatic stage is short and rapidly progressive and is associated with a 2-year survival rate of 50% or less (3–5).

Evolving Treatment Options for Severe Aortic Valve Stenosis

Traditionally, elective surgical aortic valve replacement has been considered the most effective treatment for advanced disease, significantly improving patient symptoms and survival compared with patients who are unwilling or unable to undergo surgery (6,7). Aortic valve bypass surgery, in which the left ventricular apex is connected to the descending aorta by means of a conduit valve, is also an option, although it is more rarely performed.

Unfortunately, not all patients are eligible for surgery. Several studies have identified various subgroups of patients with a substantially elevated risk for surgery-related complications or death (8–10), with some series reporting inoperability in up to 32% of cases (4). Factors contributing to a substantially increased surgical risk include frailty and old age, prior radiation therapy with significant chest damage, a heavily calcified aorta, severe pulmonary or hepatic disease, and chest deformities. Surgical risk is also increased in the presence of depressed renal function, previous stroke, peripheral vascular disease, and reduced left ventricular function. Because untreated symptomatic aortic valve stenosis has a dismal short-term prognosis, a less rigorous approach is needed for this subgroup of patients.

Teaching Point

In recent years, alternative therapeutic options for patients deemed inoperable have emerged with the development of transcatheter-based therapies and specific aortic valve prostheses that can be transported to the aortic root using a nonsurgical endovascular, transaortic, or transapical approach. Once in place, these bioprosthetic valves functionally replace the native valve by displacing it to the aortic root wall during deployment. Given its less invasive nature, this procedure is less strenuous for patients and can therefore be applied in selected patients in a nonsurgical subgroup. The procedure is known as transcatheter aortic valve replacement (TAVR), also referred to as transcatheter aortic valve implantation or percutaneous aortic valve replacement. Recently published data from individual centers, large prospective studies, observational registries, and multicenter randomized controlled trials have validated the efficacy of TAVR compared with the standard of care in patients with severe aortic valve stenosis. Therefore, TAVR is currently a valid treatment option in both the high-risk surgical cohort and the subgroup deemed to be at too high a risk for conventional surgery (11–15). These results, together with promising short- and medium-term outcomes, have led to the success and increasingly widespread clinical implementation of this intervention, with over 50,000 procedures now being performed worldwide each year (16,17). Because the clinical technique was implemented only recently, long-term outcomes are not yet known.

Nevertheless, not every patient who is refused or is at high risk for surgery is a good candidate for TAVR. A thorough clinical evaluation remains an important part of the global procedural assessment, since the overall condition of some patients may be so severely compromised by frailty, known and/or masked comorbidities, or a deteriorated mental state that even a successful TAVR procedure will have little chance of improving the patient's quality of life. Besides this clinical selection, certain technical and anatomic criteria must be met, and it is in this respect that noninvasive imaging techniques play a crucial role in the selection and further preprocedural workup of patients.

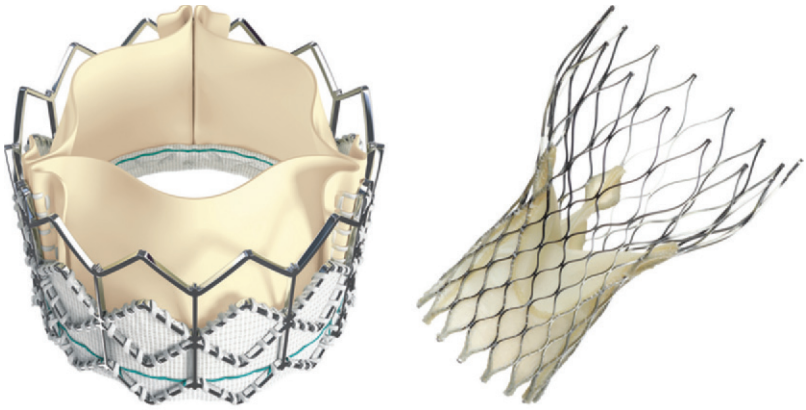

a. b.

Figure 1. Currently clinically implemented transcatheter valves. **(a)** The balloon-expandable Sapien XT valve (Edwards Lifesciences) consists of a cobalt-chromium frame and bovine pericardial leaflets. **(b)** The CoreValve (Medtronic) has a self-expanding nitinol frame and porcine pericardial leaflets.

Table 1: Overview of Sapien XT and CoreValve Transcatheter Valves and Their Respective Delivery Systems

Parameter	Sapien XT	CoreValve
Manufacturer	Edwards Lifesciences	Medtronic
Aortic annular range (mm)	18–27	18–29
Deployment	Balloon-expandable	Self-expandable
Frame	Cobalt-chromium	Nitinol
Pericardial leaflets	Bovine	Porcine
Valve function	Intraannular	Supraannular
Access routes	Transfemoral, transaortic, transapical	Transfemoral, transaortic, transaxillary
Delivery sheath size	22–24 F, 16/18 F (Novaflex +)	18 F

Definition of TAVR

The various procedural aspects of TAVR may be viewed at Movie 1 (online).

Teaching Point

Basically, a TAVR procedure consists of deploying a bioprosthetic aortic valve in the aortic root after transporting the device from a chosen entry point. The approach can be retrograde (ie, using the femoral or subclavian artery as an endovascular access point) or anterograde percutaneous transapical through the apex of the left ventricle. A suprasternal approach through the brachiocephalic trunk, an anterior approach through a minimal right anterior thoracotomy, or a partial ministernotomy for transaortic placement through the ascending aorta is also possible (18–21).

Currently, two types of transcatheter valves are commercially available for TAVR. Edwards Lifesciences (Irvine, Calif) makes the balloon-expandable Sapien and Sapien XT valves (Fig 1a). The Sapien XT valve is a slightly different version of the Sapien valve. It was introduced in Europe and features a cobalt-chromium lower-profile frame. Medtronic (Minneapolis, Minn) makes the self-expandable CoreValve revalving system (Fig 1b). These transcatheter valves have different physical properties that have been extensively described elsewhere (12,22,23). A brief summary is provided in Table 1. Both devices have been clinically implemented worldwide and have received approval from the U.S. Food and Drug Administration for the American market for use in patients with severe symptomatic aortic stenosis who are considered to be at high surgical risk or are declined for surgery owing to excessive risk.

Several device sizes exist, covering different diameter ranges of the native aortic annulus (Fig 2). With the current commercially available devices, TAVR is technically possible when the aortic annular diameter is between 18 and 29 mm (range for the two devices combined). Nevertheless, multiple vendors are currently developing other devices; thus, these size criteria will no doubt continue to evolve in the coming years.

Teaching Point

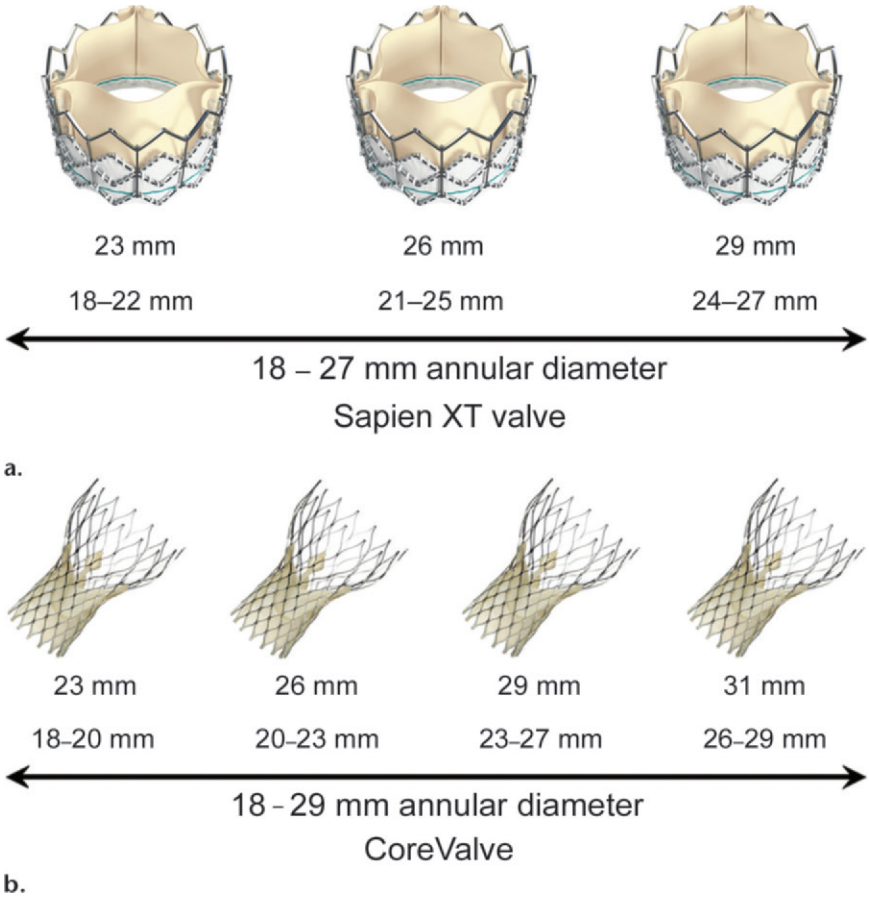

Figure 2. Available transcatheter valve sizes from Edwards Lifesciences **(a)** and Medtronic **(b)** with their corresponding ranges of aortic annular diameters. The diameter of the aortic annulus must be between 18 and 29 mm, regardless of other parameters.

Regardless of the device chosen, balloon aortic valvuloplasty is traditionally performed first, to dilate the stenotic native aortic valve and allow better passage of the transcatheter valve to its final position. Next, the position of the unexpanded prosthetic valve is checked; if this position is deemed adequate, deployment is initiated in a plane perpendicular to the aortic annular plane. The balloon-expandable Sapien valve is expanded during rapid ventricular pacing to minimize cardiac output and prevent device migration during deployment (24). Pacing is not typically performed during deployment of the CoreValve device, which has a self-expanding frame that conforms to the native aortic annulus.

Preoperative Imaging of Potential Access Routes

Importance of Preoperative Evaluation

Before the transcatheter valve is deployed in the aortic root, it must be transported to its target destination using a device-specific delivery system (Table 1). Both Sapien and CoreValve devices allow transfemoral and transaortic access. Depending on the device chosen, a transaxillary (CoreValve) or transapical (Sapien) access route is also possible. All except the transfemoral approach require a surgical incision for initial access.

The final selection of access route will depend on a combination of the device chosen, the physical properties of the corresponding delivery system, and the adequacy of the investigated pathway. A carefully chosen access route is therefore one of the key components of procedural eligibility and success, since in a given case different pathways may be associated with potentially different risks for peri- and postprocedural vascular and embolic cerebrovascular complications. This underscores the need for individualized access route selection.

Teaching Point

Both device- and anatomy-related obstacles may alter the chosen access pathway or even make the procedure impossible to perform via the endovascular pathway regardless of device-compatible aortic root dimensions (Fig 3) (24). Therefore, multidetector CT plays an important role in examining the potential access routes and

a. b.

Figure 3. Inadequate access route patency. **(a)** Maximum intensity projection CT angiographic image reveals a subocclusive stenosis in the right external iliac artery (arrow) inhibiting endovascular access through the right iliac arterial axis, with diffuse atherosclerotic calcifications in the other aortoiliac vessels. **(b)** Volume-rendered CT image obtained in a different patient shows general tortuosity of the aortoiliac arterial vessels, a finding that is most prominent in the left common iliac artery (arrow).

reporting any possible problems that may alter the chosen access strategy (24,25).

Endovascular Access

Commercially available device delivery systems come with different sheath sizes depending on the manufacturer and the production version of the device. Ideally, the minimum diameter of the native vessel should be smaller than the outer diameter of the chosen delivery sheath (Table 1). Lower-profile sheaths and delivery catheters improve procedural safety and expand patient eligibility. Currently, the two systems associated with the most worldwide experience and reported study results are *(a)* the third-generation femoral delivery systems from Medtronic, with a sheath size of 18 F (26); and *(b)* the Edwards Lifesciences Retroflex, with a 22–24-F sheath (27). Edwards Lifesciences has also created the Novaflex+ transfemoral delivery system with a 16/18-F low-profile introductory sheath. However, delivery catheters remain the subject of intense research and have been continuously improved ever since their introduction, with other systems currently being developed by different vendors.

Not surprisingly, a larger sheath size (22–24 F) has been associated with a higher incidence of vascular complications (22.9%–30.7%) (12,28) compared with smaller systems (1.9%–13.3%) (29,30). To allow proper tracking and meaningful comparisons of endpoints in trials, major and minor vascular complications have been formally defined by the Valve Academic Research Consortium (31). Prominent atherosclerotic (specifically, circumferential) wall calcifications, small native vessel diameter (smaller than the outer diameter of the delivery sheath being used), and marked tortuosity of the iliac arteries have been described as risk factors for procedural complications (Fig 3) (24,32), with some series finding an unsuitable iliofemoral anatomy in 19.1%–35% of patients (32–34). When two or more of these features are present, an alternative transapical, transaxillary, or transaortic approach can be considered (24). Hayashida et al (35) proposed the ratio of sheath size to femoral artery size (SFAR) as the most predictive variable in identifying patients at risk for vascular access injury. With use of a SFAR sliding scale depending on the burden of atherosclerotic calcification, a threshold of 1.05 was predictive of a higher rate of major complications as defined by the Valve Academic Research Consortium. Therefore, the authors suggest that routine application of SFAR improves patient selection, leads to better outcomes, and lowers the morbidity profile for TAVR (35). The minimum recommended vessel diameters are shown in Table 2 (36).

Table 2: Recommended Minimum Vessel Diameter based on the Delivery Device

Device	Valve Size (mm)	Introducer Profile (mm)	Recommended Minimum Vessel Diameter (mm)
Sapien valve with Retroflex 3-mm delivery system	23	22	>7
	26	24	≥8
Sapien XT valve with Novaflex delivery system and e-sheath	23	16	≥6
	26	18	≥6.5
	29	20	≥7
CoreValve revalving system	23	18	≥6
	26	18	≥6
	29	18	≥6
	31	18	≥6

Note.—Adapted, with permission, from reference 36.

Information regarding the patency of the chosen endovascular route can be acquired during preprocedural evaluation with multidetector CT and conventional coronary angiography, but it can also be obtained from previous imaging studies (sometimes performed for unrelated reasons). Although there are no guidelines regarding how recent such a study should be, we believe that a study should have been performed no more than 6 months ago, unless there are clinical grounds for a recent change in vascular status.

Conventional coronary angiography is always routinely performed at our institution in potential TAVR candidates for whom recent information about coronary patency is not available. In such cases, this examination is expanded to include an assessment of the aorta and iliac arteries.

Although conventional angiography allows a basic assessment of the luminal size of the involved peripheral arteries, it is less suitable for optimal assessment of the presence, amount, and morphologic features of atherosclerotic calcifications and vessel tortuosity. Multidetector CT is therefore considered a valuable tool for vascular assessment due to its intrinsic cross-sectional and three-dimensional (3D) multiplanar capabilities. In practice, precise multidetector CT–derived measurements of the common femoral, external iliac, and common iliac arteries are obtained at several levels using curved multiplanar reformation, measuring the transaxial diameter on a view obtained perpendicular to the long axis of the investigated vessel segment. Although there are no universally accepted guidelines regarding the anatomic level at which measurements along a vessel trajectory should be obtained, it is important to choose the measurement points so that information can be acquired concerning both average vessel diameter and narrow segments that may hinder passage of the transcatheter device. This information is relevant, since TAVR procedures have been successfully performed in patients with borderline vessel size and in those without extensive atherosclerotic burden or tortuosity but with relatively compliant arteries with a short-segment diameter up to 1–2 mm smaller than the intended sheath size (24,33,37). The degree of atherosclerosis remains a subjective matter, with no quantifiable parameters or published guidelines, and is therefore subject to interpretation by the radiologist, cardiologist, and cardiovascular surgeon. An accurate and complete description of the degree of atherosclerotic burden by the radiologist is therefore necessary and should include the presence and extent of atherosclerotic plaques and stenosis (20). Finally, we routinely obtain 3D volume-rendered images of the aortoiliac arteries for further subjective evaluation of vessel tortuosity and general morphology.

Both left and right subclavian arteries may be used for endovascular access with a transaxillary approach. However, the left subclavian artery is often preferred because, similar to the femoral artery, it allows a more favorable orientation of the delivery system. Furthermore, a left-sided approach will minimize the potential obstructive effect of the delivery system on the ostium of the brachiocephalic artery and the subsequent risk of stroke (20). Nevertheless, caution is needed to prevent vascular complications such as dissection or occlusion of the vessels of the arm and head. Ipsilateral transvenous internal pacemaker leads and internal mammary artery grafts are not considered contraindications but do increase procedural complexity. Finally, some centers have experience—albeit limited—with a suprasternal approach through the brachiocephalic trunk (21).

Transaortic Access

Worldwide experience with the transaortic approach through an anterior right mini–thoracotomy or partial mini–sternotomy is increasing

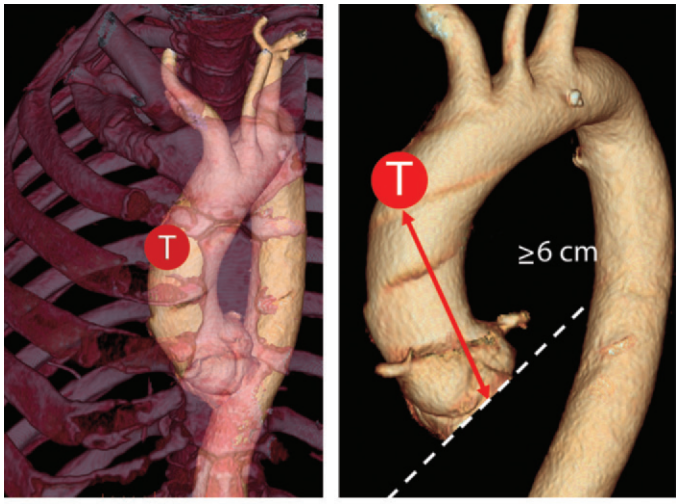

a. b.

Figure 4. Entry site for transaortic access for TAVR. **(a)** Volume-rendered CT image shows the approximate target point *(T)* for transaortic access through a minimal right sternotomy or thoracotomy, typically located at the level of the second intercostal space. **(b)** For CoreValve devices (Medtronic), a minimum distance of 6 cm (double-headed arrow) between the entry point *(T)* and the aortic annular plane (dashed line) is recommended to accommodate the device length.

(Fig 4). Access is typically achieved at the level of the second right intercostal space, bypassing the aforementioned peripheral vascular territories and thereby providing an alternative route when other approaches have been deemed unsuitable. At our institution, this procedure has been well tolerated by patients. As more experience with this access pathway is gained, the potential problem of not having an adequate endovascular access pathway is becoming less of an issue. However, the transaortic approach also has certain anatomic requirements, including a minimum distance of 6 cm between the basal aortic plane and the aortic access site for CoreValve implantation. Further preoperative CT evaluation for transaortic access must also include analysis of the selected delivery trajectory to optimize coaxial alignment with the native aortic valve, evaluation of the presence of calcification at the aortic access site, and correct identification of critical vessels such as the right internal mammary artery and possible bypass grafts along the delivery trajectory. Concomitant pleural or lung parenchymal disease along the delivery trajectory as well as other unexpected findings may further compromise this entry point. Currently, there are no guidelines as to which lung diseases exclude this procedure, with the final decision being left to the interventional cardiologist and surgeon.

Although in practice aortic disease will be less critical in determining procedural feasibility, several procedural contraindications involving aortic disease have been described. These include severe aortic angulation, coarctation, aneurysm of the abdominal aorta with protruding mural thrombus, and previous aortofemoral bypass surgery (38).

CT Acquisition

Required Anatomic Coverage and Preoperative Information

In practice, the CT scanning protocol will be determined mainly on the basis of the required preoperative information, the patient's condition, and the need to reduce the required amount of contrast material. The last-named factor is especially important in the investigated population, since advanced age is often associated with depressed renal function. An overview of the required multidetector CT information is given in Table 3.

In general, the technical multidetector CT settings used for routine CT angiography of the coronary arteries constitute an excellent starting point. Next, the required scanning range should be determined. When only information concerning the aortic root is required, many centers use electrocardiography (ECG)–gated contrast material–enhanced multidetector CT of the heart with a scanning range identical to that used for routine multidetector CT of the coronary arteries. However, it can be argued that, especially in patients with impaired renal function, acquisition can be limited to the aortic root, since evaluating the status of the coronary

Table 3: Required Information from Preprocedural CT Examinations

Anatomic Level	Required Information
Aortic annulus	Systolic measurements (if available) are preferred Annular cross-sectional (long- and short-axis) diameters, circumference, and area; circumference- and area-derived diameters Recommended fluoroscopic projection angle for orthogonal view in annular plane if not determined during procedure (eg, at 3D rotational angiography)
Aortic valve (native)	Extent and distribution of valve calcifications, cuspidity (bicuspid, tricuspid, other variants)
Aortic root	Shortest distance from aortic annulus to ostia of left main and right coronary arteries
Left atrium	Exclusion of a left atrial appendage thrombus with either TEE or delayed phase imaging
Left ventricle	Evaluation for basal septal hypertrophy and wall thrombi
Ascending aorta	Extent of wall calcifications (especially if a transaortic approach is being considered) and presence or absence of atherosclerotic thrombi, angulation between ascending aorta and LVOT
Aortic arch, descending aorta, and abdominal aorta	Branch anatomy of aortic arch (subclavian approach), descriptive assessment of atherosclerosis (including tortuosity, intraluminal obstruction, and thrombi)
Subclavian arteries and brachiocephalic artery	Report on patency and luminal diameter (left subclavian artery is preferred)
Common and external iliac arteries and common femoral artery	Report on patency and luminal diameter, descriptive assessment of atherosclerosis (including tortuosity), report of any potential problems at the targeted femoral access site (eg, preexisting pseudoaneurysm)

Note.—TEE = transesophageal echocardiography.

arteries is not the purpose of the multidetector CT examination. Limiting the investigated anatomic range and acquisition time to the bare minimum allows a reduction in the required amount of intravenous contrast material. If evaluation of the patency of the subclavian arteries is also required, the scanning range should extend from the neck base to the thoracic diaphragm.

When evaluation of the iliac access route is also requested, the scanning protocol is also influenced by the acquisition speed of the available multidetector CT equipment, since this anatomic region is farther away from the aortic root. Last-generation multidetector CT scanners with a large anatomic coverage per rotation and/or high pitch modes will allow scanning of both the heart and aortoiliac vessels within a minimum time span and with a single reduced dose of contrast material (39–41). With slower multidetector CT scanners, it may be necessary to perform two different multidetector CT examinations on separate days to achieve optimal arterial enhancement of the targeted vascular territory. At our institution, using a single-source 64-section multidetector CT system (Lightspeed 64; GE Healthcare, Milwaukee, Wis), we combine two different but consecutive acquisitions during the same intravenous contrast material injection, as was also proposed by Blanke et al (39). First, a retrospectively ECG-triggered examination is performed, with anatomic coverage limited to the region of the aortic root. A nongated examination is subsequently performed from a supraclavicular level to below the common femoral artery. We administer a single 120-mL dose of contrast material with a high iodine concentration (a minimum of 350 mg/mL is recommended).

Using this approach, we combine the flexibility of ECG-triggered acquisition for optimal-quality images of the aortic root with a subsequent faster scan for evaluation of the pathways of the subclavian and iliac arteries. In addition, we routinely use 80 or 100 kV as the default setting (depending on body weight), since lower kilovolt settings have been shown to reduce radiation dose for multidetector CT angiography without compromising image quality (42).

Finally, atrial fibrillation is a known risk factor for the development of atrial thrombi, especially in the left atrial appendage. This is particularly important because the presence of thrombus in the left atrium is a procedural contraindication with an increased peri- and postprocedural risk of stroke (Fig 5). Although echocardiography has traditionally been the preferred modality for screening for this abnormality, atrial thrombi can be detected with contrast-enhanced multidetector CT and should always be mentioned in the radiology report (43). However, caution should be exercised when evaluating the left atrial ap-

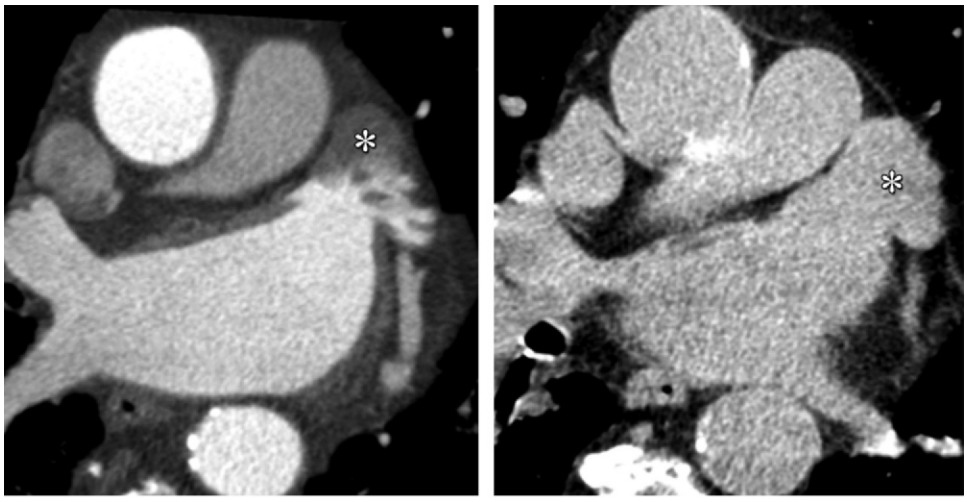

a. b.

Figure 5. Circulatory stasis in a large left atrial appendage producing a pseudothrombus during pre-TAVR evaluation. **(a)** Axial contrast-enhanced CT image demonstrates how slow flow can lead to incomplete filling of the left atrial appendage (*) during the arterial phase. When detected, an atrial appendage thrombus must be either confirmed or excluded. This is traditionally achieved with TEE, although delayed phase CT images can also be used. **(b)** Axial contrast-enhanced delayed venous phase CT image shows final complete filling of the appendage (*). The possibility of a left atrial appendage thrombus must always be reported immediately, since such a finding constitutes a procedural contraindication with a high risk of stroke.

pendage on single-phase arterial scans, since circulatory stasis in a large appendage can produce a false-positive pseudothrombus. Performing a dual-phase examination with images acquired in a delayed contrast phase increases the sensitivity and specificity of CT for this abnormality (43). In our practice, we quickly review the incoming arterial phase images as they appear on the CT console, and when incomplete filling of the left atrial appendage is observed, an additional targeted scan is performed, typically an average of 2 minutes after contrast material injection.

ECG Gating and the Varying Dimensions of the Aortic Annulus during the Cardiac Cycle

Given the inherent motion of the aortic root, an ECG-gated multidetector CT acquisition is necessary to achieve the best image quality with minimal motion artifacts. It also allows evaluation of the dimensions of the aortic root, which vary depending on the phase of the cardiac cycle. The aortic annulus is traditionally measured in the systolic phase, during which it manifests with its intrinsically largest diameter**.** Nevertheless, several authors have reported varying results concerning the optimal scanning window in the cardiac cycle. A multidetector CT–based study in healthy subjects reported a significant difference in the dimensions of the aortic annulus between systole and diastole (up to 5 mm in some cases) (44). However, this is a different patient population than that with severely stenotic aortic valves, in which this variation is thought by some investigators to be minimal due to reduced wall compliance (45–47). Nevertheless, Hamdan et al (48), using four-dimensional multidetector CT data, reported that in both healthy subjects and patients with calcified aortic valves, the aortic annulus was generally elliptic but assumed a more round shape in systole, thereby increasing the minimum diameter but without a significant change in perimeter. On the basis of these findings and our own experience, we generally recommend ECG-triggered scanning of the aortic root with systolic measurements. Consequently, ECG-modulated milliamperage settings should be adjusted to deliver sufficient image quality in the systolic phase.

Still, ECG gating by itself can also induce artifacts. In practice, this implies that on most equipment, the best image quality will be achieved in patients with a slow and regular heartbeat. However, because the investigated cohort is almost invariably of advanced age with an associated higher incidence of significant comorbidity, the measures that are typically used to lower the heart rate (eg, the administration of additional β-blockers) are not always possible or are less clearly indicated. Moreover, the presence of atrial fibrillation is not rare in an advanced-age population, further adding to the technical complexity of acquiring high-quality images.

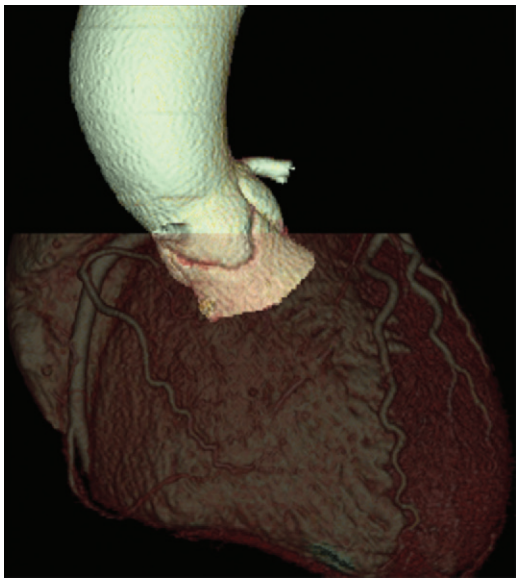

Figure 6. Volume-rendered CT image shows the central position and oblique angulation of the aortic root and annular plane.

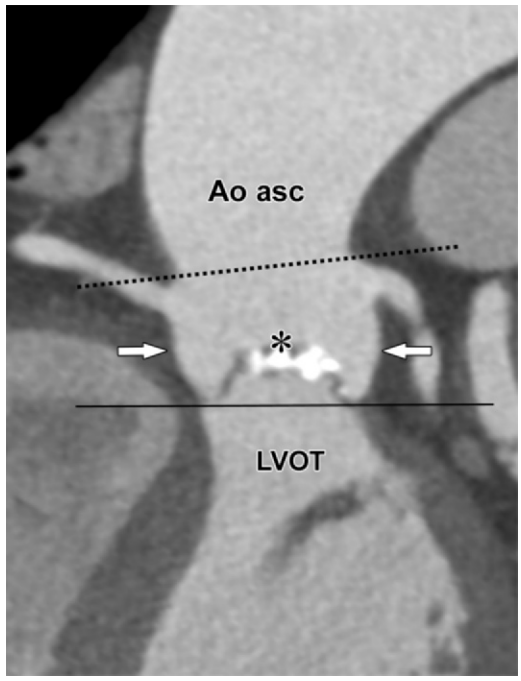

Figure 7. Coronal contrast-enhanced CT image shows the aortic root extending between the LVOT and the ascending aorta *(Ao asc)*, with its borders formed by the sinotubular junction (dashed line) and the basal attachments of the aortic valve leaflets, which define the level of the annular plane (solid line). The aortic root contains the sinus of Valsalva (arrows) and aortic valve leaflets (*).

Clinically Relevant Anatomy

The aortic root has a relatively central position in the heart, with a double-oblique orientation at 3D imaging (Fig 6). It extends from the LVOT to the sinotubular junction, which marks the transition from the aortic sinuses (of Valsalva) to the tubular ascending aorta. This junction can be identified as an area of abrupt change in caliber, better seen on coronal and sagittal reformatted images as an obtuse angulation. The aortic root also contains the aortic valve within the aortic sinus (Fig 7). Three distinct aortic valve leaflets can be visualized, with left and right coronary cusps named after the corresponding coronary arteries originating from their sinuses. A third cusp is appropriately named the noncoronary cusp, since no coronary artery originates from its sinus (Fig 8).

In contrast to these anatomic landmarks, the aortic annulus is not a real anatomic structure. Instead, the term *aortic annulus* is often used by surgeons to refer to the insertion site of the aortic valve cusps, which many authors have traditionally assumed is always circular (49,50). Nevertheless, this term is not adequately defined anatomically, with a nonstandard and variable interpretation. Consequently, some authors have suggested refraining from using the term (51). Still, its use is widespread and deeply embedded in scientific literature and communications.

In practice, the term *annulus* is commonly used to specifically indicate a virtual ring formed by the nadir of the attachment sites of the aortic valve leaflets. This attachment of the aortic valve leaflets to the aortic root wall is not circular; it has a more semilunar, crown-shaped appearance, ex-

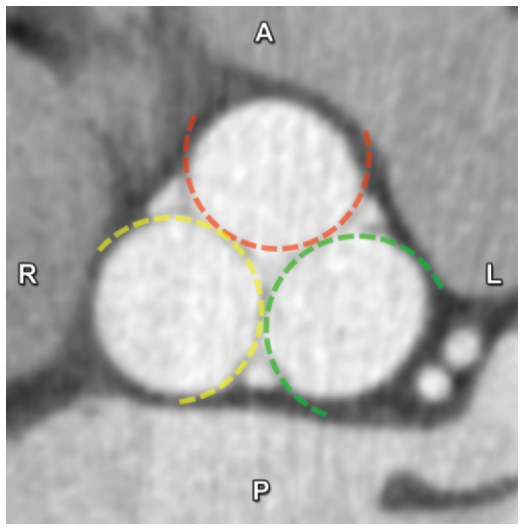

Figure 8. Double-oblique contrast-enhanced CT image of the aortic root at the level of the sinuses of Valsalva demonstrates the anatomy of the aortic valve, consisting of left coronary (green), right coronary (red), and noncoronary (yellow) cusps. Note the cloverleaf shape of the aortic root contour. *A* = anterior, *P* = posterior.

tending from the sinotubular junction to the basal attachment plane of the aortic valve leaflets (the so-called annulus), located just below the ventriculoarterial junction. Given its conical form, the annulus is perhaps more appropriately described as a three-pronged coronet than as a ring.

Histologically, the aortic root consists of a ventricular component (at the level of the membranous septum) and an arterial component as the leaflet insertions extend up to the sinotubular junction (49,50).

At cross-sectional imaging, the aortic root contour is practically circular at the level of the sinotubular junction and assumes a more cloverleaf shape at the level of the aortic sinus, often becoming oval to ellipsoid at the annular plane and LVOT (Fig 9). Consequently, small differences in the choice of a measurement plane in the aortic root can produce notably different results.

Noninvasive Imaging of the Annulus: Ongoing Controversies and Current Insights

Multimodality Imaging Comparison

With TAVR, unlike with surgical valve replacement, annular sizing is not performed under direct inspection but on the basis of noninvasive imaging findings. Imaging guidance is needed to ensure the appropriate degree of oversizing to help avoid paravalvular regurgitation and reduce the potential risk of annular rupture.

Historically, transthoracic echocardiography (TTE) and TEE have been used for preoperative sizing of the aortic annulus in different trials. However, because they are operator-dependent two-dimensional (2D) imaging techniques, they provide only limited data regarding the complex 3D geometry of the annulus (Figs 10, 11). Because of the noncircular nature of the annulus and the fact that echocardiography typically yields measurements that most closely approximate the short axis of the annulus, TEE measurements have been shown to understate the surgically measured annular size (52).

To further optimize the sizing process, the potential contributions of 3D imaging methods such as multidetector CT, 3D TEE, and (potentially) 3D rotational angiography have recently been fairly extensively investigated (24,53–56). Multidetector CT, with its isotropic voxels and multiplanar reformatting capabilities, seems intrinsically better suited than echocardiography for correctly characterizing the complex 3D anatomy of the aortic annulus. As such, it allows reconstruction of the dataset in the true plane of the aortic annulus, after which various measurements of the annulus can be obtained.

MR imaging is also increasingly being used for the evaluation of the aortic valve area, with encouraging results (57–59), and, according to some authors, yields measurements comparable to those obtained with multidetector CT (60). In some respects, MR imaging of the aortic root has clear benefits compared with multidetector CT, including *(a)* radiation-free imaging, *(b)* functional evaluation of the aortic valve, and *(c)* the use of gadolinium-based contrast material, which is significantly less nephrotoxic and produces less adverse reactions than its iodine-based multidetector CT counterpart. Nevertheless, the use of MR imaging is far less widespread than that of multidetector CT for obtaining annular measurements, probably because (among other reasons) MR imaging is a technically more complex examination, takes a longer time, and requires a higher degree of patient cooperation. However, on a case-by-case basis, MR imaging may be used instead of multidetector CT in patients with severely depressed renal function.

Nevertheless, comparisons between imaging methods are often the subject of debate, since experience with MR imaging and multidetector CT as selection and sizing tools is of fairly recent origin (24,58,60–62). As a result, there are currently no universally validated strict guidelines regarding the exact use of multidetector CT or any other 3D imaging tool for patient selection and device sizing across all platforms. Therefore, it is important to realize that in practice, the process of clinical patient evaluation, annular sizing, and evaluation of access route for final transcatheter heart valve selection and placement is multifactorial, integrating both clinical data and information from all available imaging modalities. This approach allows the most complete clinical and technical assessment, leading to an informed procedure and optimal device selection.

Teaching Point

Paravalvular Regurgitation and the Importance of the Correct Assessment of Annular Dimensions

Proper selection of a patient on clinical grounds (overall assessment of frailty and comorbidity factors, which influence life expectancy and the ability to undergo TAVR) and correct choice of a patient-specific transcatheter valve size are crucial for successful TAVR, minimizing peri- and postprocedural complications. Postprocedural regurgitant leakage of blood around the attachment sites of the prosthetic valve remains a relatively common complication with potential important clinical consequences. This regurgitant flow is called paravalvular aortic regurgitation (PAR), with approximately one in nine patients

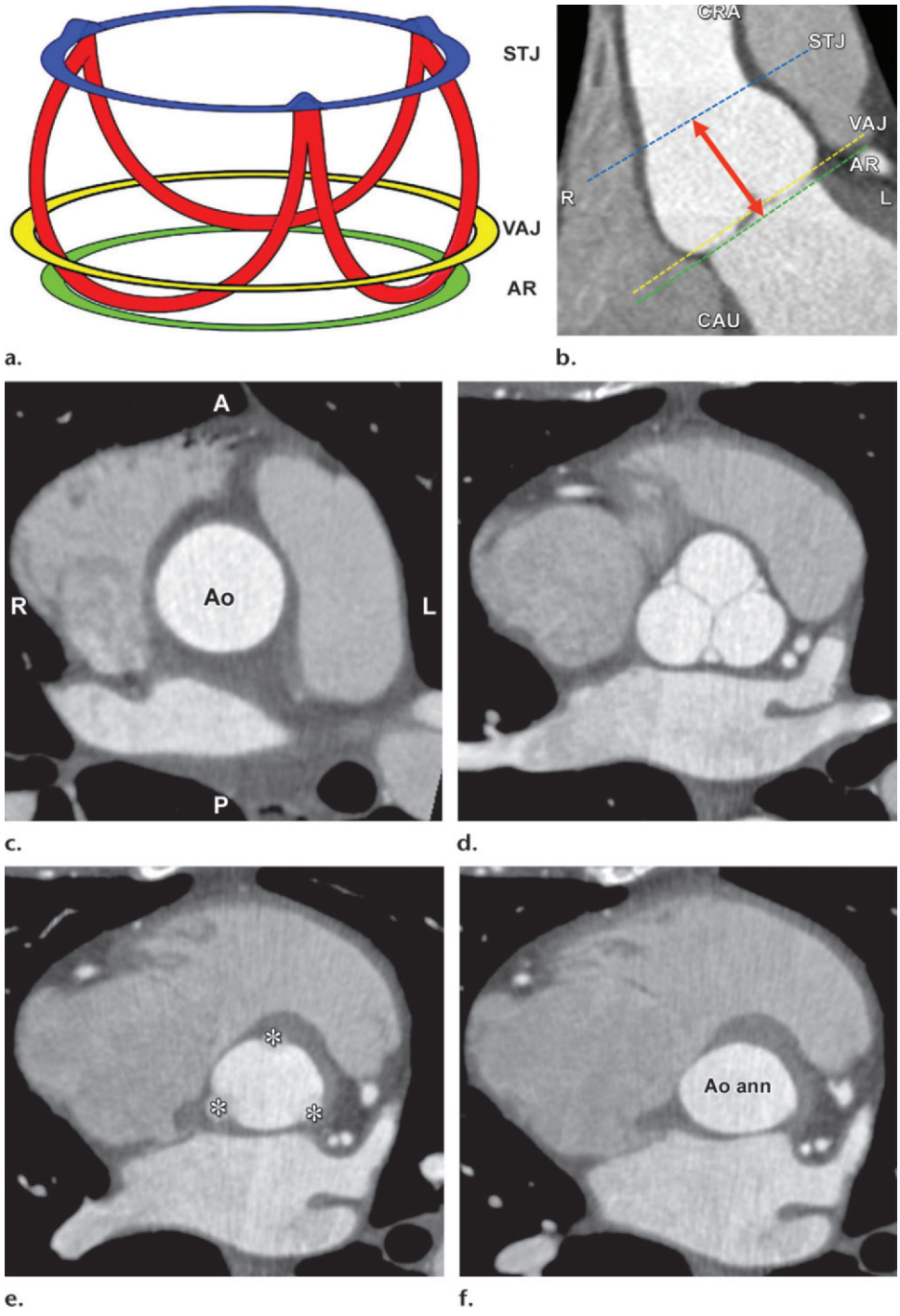

developing moderate to severe PAR after TAVR (12). PAR has also been associated with a worse long-term outcome (63). There is growing evidence that PAR may be related, at least in part, to preoperative undersizing of the aortic annulus, with the subsequent choice of an undersized transcatheter valve and incorrect device positioning (64–66). Furthermore, recent reports indicate that even mild PAR, which is generally considered to be of little clinical significance, is nevertheless an underappreciated contributor to late all-cause mortality (16).

As a result, a great deal of attention is being given to further refining annular sizing and subsequent transcatheter valve selection to help minimize the occurrence of moderate to severe PAR.

Annular Measurements and Multidetector CT: Workflow and Current Viewpoints

The primary uses of multidetector CT in annular sizing are *(a)* obtaining a correct image orientation in the true plane of the aortic annulus, *(b)* correctly measuring the annulus using

Figure 9. **(a)** Drawing illustrates the crownlike suspension of the aortic valve leaflets within the aortic root extending across the length of the aortic sinus. *AR* = virtual annular ring (green), formed by joining the basal attachments of the aortic valve leaflets; *STJ* = sinotubular junction (blue); *VAJ* = ventriculoarterial junction (yellow). Red = aortic leaflet insertion sites in the sinus of Valsalva forming a crownlike ring. (Reprinted, with permission, from reference 39.) **(b)** Coronal contrast-enhanced CT image demonstrates the levels of the sinotubular junction *(STJ)* (blue line), ventriculoarterial junction *(VAJ)* (yellow line), and annular ring *(AR)* (green line). Double-headed arrow = anatomic range of the sinuses of Valsalva. *CAU* = caudal, *CRA* = cranial. **(c–f)** Double-oblique reformatted images further clarify the changing shape of the aortic root contour. **(c)** The sinotubular junction forms the top of the crown, where the outlet of the aortic root in the ascending aorta *(Ao)* is a true circle. *A* = anterior, *P* = posterior. **(d)** The aortic root gradually becomes less circular, with a more cloverleaf shape at its midportion (ie, at the sinuses of Valsalva). At this level, the aortic valve leaflets are clearly seen. **(e)** The aortic valve leaflets (*) are just barely visible at the level of the ventriculoarterial junction, where the left ventricular structures give rise to the fibroelastic walls of the aortic valvar sinuses. Note that the aortic root contour is now becoming increasingly ellipsoid. **(f)** The bottom of the aortic root is formed by the virtual ring, or aortic annulus *(Ao ann)*, which has an oval shape in most patients.

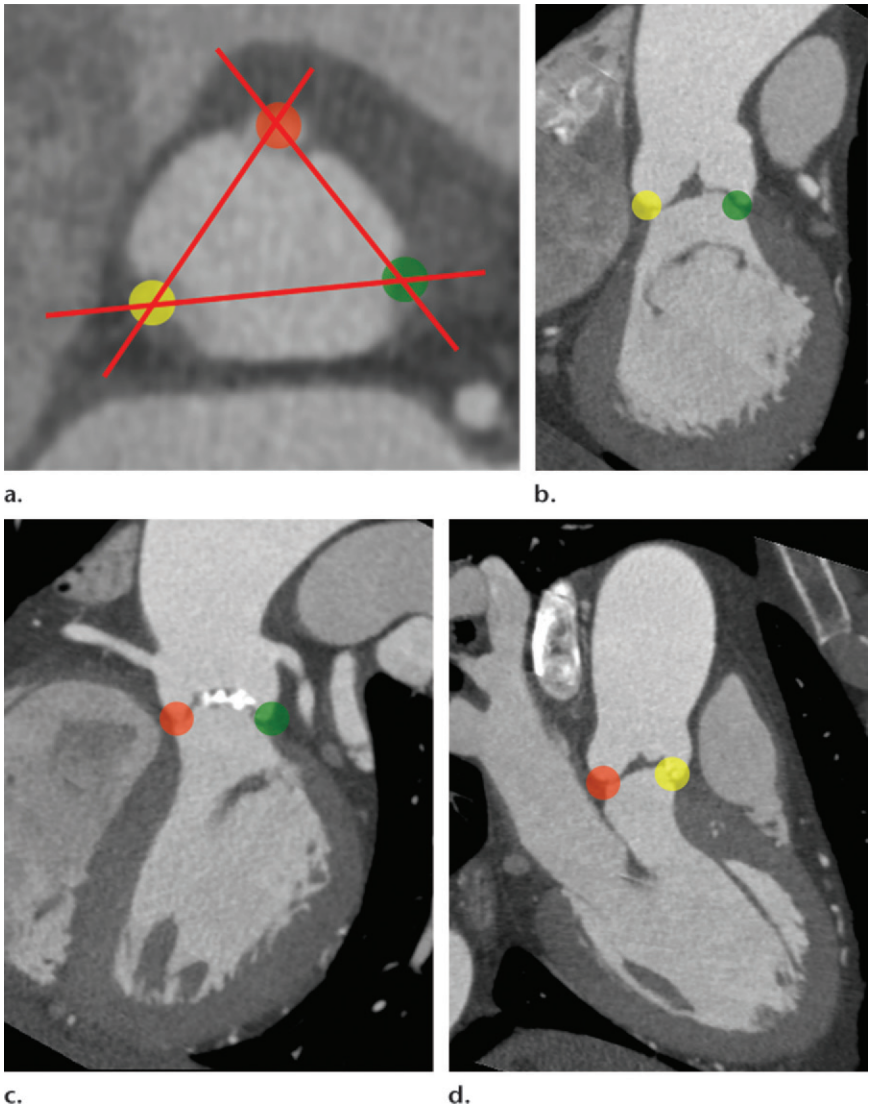

Figure 10. Double-oblique reformatted CT images show the basal insertion sites of the right coronary cusp (orange dot), noncoronary cusp (yellow dot), and left coronary cusp (green dot). When these basal leaflet insertion sites are used as a reference for deriving a single 2D measurement of the annular plane (as in 2D echocardiography-derived measurements), the 3D anatomy is reduced to a 2D image. Furthermore, these images illustrate that none of the performed 2D measurements is along the true long or short axis of the aortic annulus, complicating simple comparisons between CT and echocardiographic measurements.

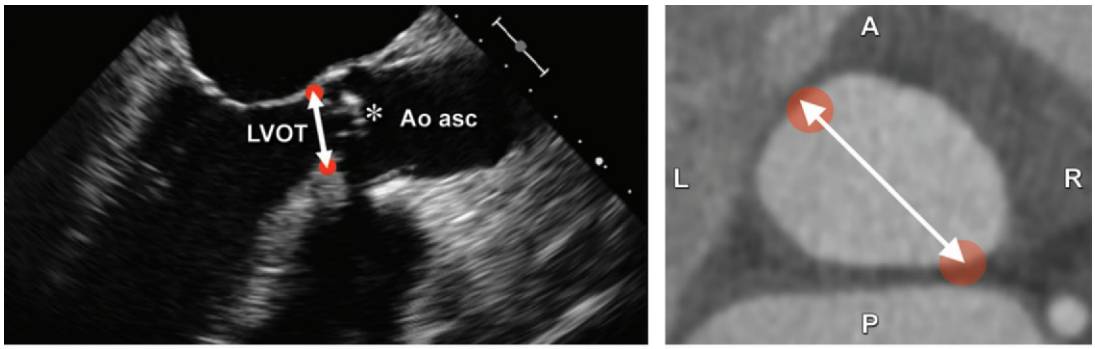

a. b.

Figure 11. **(a)** On an echocardiographic image, the diameter of the aortic annulus (double-headed arrow) is measured by identifying two opposing points (orange dots) on the basal insertion sites of the aortic valve leaflets (*). *Ao asc* = ascending aorta. **(b)** Corresponding double-oblique reformatted image through the aortic annulus reveals that the pathway (double-headed arrow) between these points (orange dots) does not correspond to the true long axis of the aortic annulus. Echocardiography-derived measurements often lead to underestimation of the true size of the annulus. Furthermore, because conventional echocardiography is a 2D imaging modality with a varying degree of operator dependency, it is almost impossible to compare single echocardiography-derived measurements with their CT counterparts, since both the measurement plane and the chosen oblique diameter will differ between these imaging modalities. *A* = anterior, *P* = posterior.

different methods, and *(c)* implementing these measurements in the selection of a transcatheter valve size.

The plane of the aortic annulus is defined by the three lowest insertion points of the aortic valve leaflets. Because this plane has a double-oblique orientation, standard coronal, sagittal, or even single-oblique reformatted images are not considered suitable. Furthermore, the insertion of the right coronary cusp leaflet is often inferior to those of the left and noncoronary cusp leaflets (36). Although these characteristics can make obtaining a correctly oriented image plane less straightforward and somewhat frustrating in inexperienced hands, a method describing a sequence of image reformations leading to an image plane precisely oriented along the aortic annulus has been described elsewhere (36). In this plane, the three lowest anchor points of the aortic valve leaflets are displayed on the same image.

Once a suitable plane has been obtained, several annular measurements can be taken. Investigators have approached annular sizing using various measurements of the annulus (Table 4). Currently, we propose calculating the mean annular diameter (preferably on the basis of systolic images) as follows (Fig 12): First, we obtain annular cross-sectional long-axis (D_L) and short-axis (D_S) diameters. The annular perimeter is manually tracked using a planimetry tool on a workstation, after which the area *(A)* and circumference *(C)* of the aortic annulus are derived by the workstation software. Finally, the mean annular diameter *(D)* is calculated based on these measurements. For the cross-sectional derived mean diameter (D_{CS}), this is carried out with simple averaging: $D_{CS} = (D_L + D_S)/2$. The area-derived (D_A) and circumference-derived (D_C) diameters are calculated as follows: $D_A = 2 \times \sqrt{(A/\pi)}$, and $D_C = C/\pi$. However, it is important to realize that D_C and D_A are calculated under the assumption that the annulus is fully circular after device deployment, particularly with balloon-expandable valves. The discrepancy between these three measurements (D_{CS}, D_A, and D_C) will therefore increase with remaining annular eccentricity, most notably with the circumference-based method. This further underscores the fact that transcatheter valve size selection is closely tied to the type of device used.

Finally, these measurements must be incorporated into the transcatheter valve size selection process. Both Medtronic and Edwards Lifesciences have provided guidelines for valve size selection that depend on annular dimensions (Fig 2). However, these sizing scales are historically based on echocardiography-derived 2D measurements of the annulus. Therefore, these manufacturer-based recommendations cannot simply be applied to multidetector CT–derived measurements without modification (67). Several studies have reported that the exclusive use of multidetector CT with an unmodified scale would influence patient eligibility and lead to the choice of a different transcatheter valve size compared with echocardiography in up to 40% of cases (24,62,68,69).

These early data led to significant confusion regarding the appropriate integration of multidetector CT measurements in annular sizing and valve selection. To help mitigate this confusion, several investigators have sought to validate

Table 4: Overview of the Heterogeneity in Methods of Obtaining Annular Dimensions across Several Studies

Authors/Year	No. of Patients	Method of Measurement at CT	CT Measurement (mm)	TTE Measurement (mm)	TEE Measurement (mm)
Yano et al/2012	55	Largest LVOT diameter	23.9 ± 3.19	20.3 ± 2.5	. . .
Altiok et al/2011	49	Coronal and sagittal aortic annular diameters	Coronal: 22.19 ± 1.96 Sagittal: 22.27 ± 2.01	. . .	Coronal: 23.6 ± 1.89 Sagittal: 23.46 ± 2.07
Pontone et al/2011	60	Maximum and minimum aortic annular diameters	Maximum: 25.1 ± 2.8 Minimum: 21.2 ± 2.2	21.6 ± 1.4	20.9 ± 2.0
Tzikas et al/2011	70	Coronal, sagittal, and mean aortic annular diameters	Coronal: 26.3 Sagittal: 21.8 Mean: 23.7	22.6	. . .
Dashkevich et al/2011	33	Mean aortic annular diameter	24.5 ± 2.6	. . .	23.4 ± 2.4
Mizia-stec et al/2011	20	Mean aortic annular diameter	26.9 ± 3.2	24 ± 3.6	26 ± 4.2
Messika-Zeitoun et al/2010	45	Long-axis, short-axis, and mean aortic annular diameters	Long-axis: 27.5 ± 3.1 Short-axis: 21.7 ± 2.3 Mean: 24.6 ± 2.4	23.1 ± 2.1	24.1 ± 2.1
Delgado et al/2010	53	Annular area measured with planimetry	4.65 ± 0.82*	3.89 ± 0.74*	Planimetry: 4.22 ± 0.77* Circular: 4.06 ± 0.79*
Halpern et al/2009	41	Aortic valve area measured with planimetry	3.1 ± 1.4*	2.5 ± 1.3*	. . .
Wood et al/2009	44	Coronal and sagittal aortic annular diameters in systole/diastole	Coronal: 25.7 ± 1.5 /25.5 ± 2.5 Sagittal: 22.4 ± 1.3 /21.5 ± 2.1	. . .	. . .
Tops et al/2008	169	Coronal and sagittal aortic annular diameters	Coronal: 26.3 ± 2.8 Sagittal: 23.5 ± 2.7	. . .	. . .
Willmann et al/2002	25	Mean aortic annular diameter	24.0 ± 2	. . .	. . .

Note.—When available, the corresponding echocardiography-derived measurements are obtained.
*Units are in square centimeters.

multidetector CT–based sizing guidelines for both the self-expanding and balloon-expandable platforms.

For balloon-expandable valves, Gurvitch et al (67) have provided an early modified sizing-scale proposal based on the cross-sectional mean annular diameter, the area-derived mean diameter, and the expected differences between these multidetector CT–based diameters and the echocardiographic measurements. Using this modified scale, they found that the multidetector CT–based measurements would modify valve selection in only about 10% of patients, all of whom had moderate to severe PAR after a device size had been selected based on echocardiographic measurements (67). This suggests that multidetector CT can help in further reducing PAR in those cases in which echocardiography did not help identify the optimal valve size. On the basis of these findings and other retrospective analyses, Willson et al (70) recently proposed a multidetector CT–based annular area sizing scheme with the goal of achieving an annular area oversizing of 10%. This sizing algorithm has recently been validated in a multicenter trial

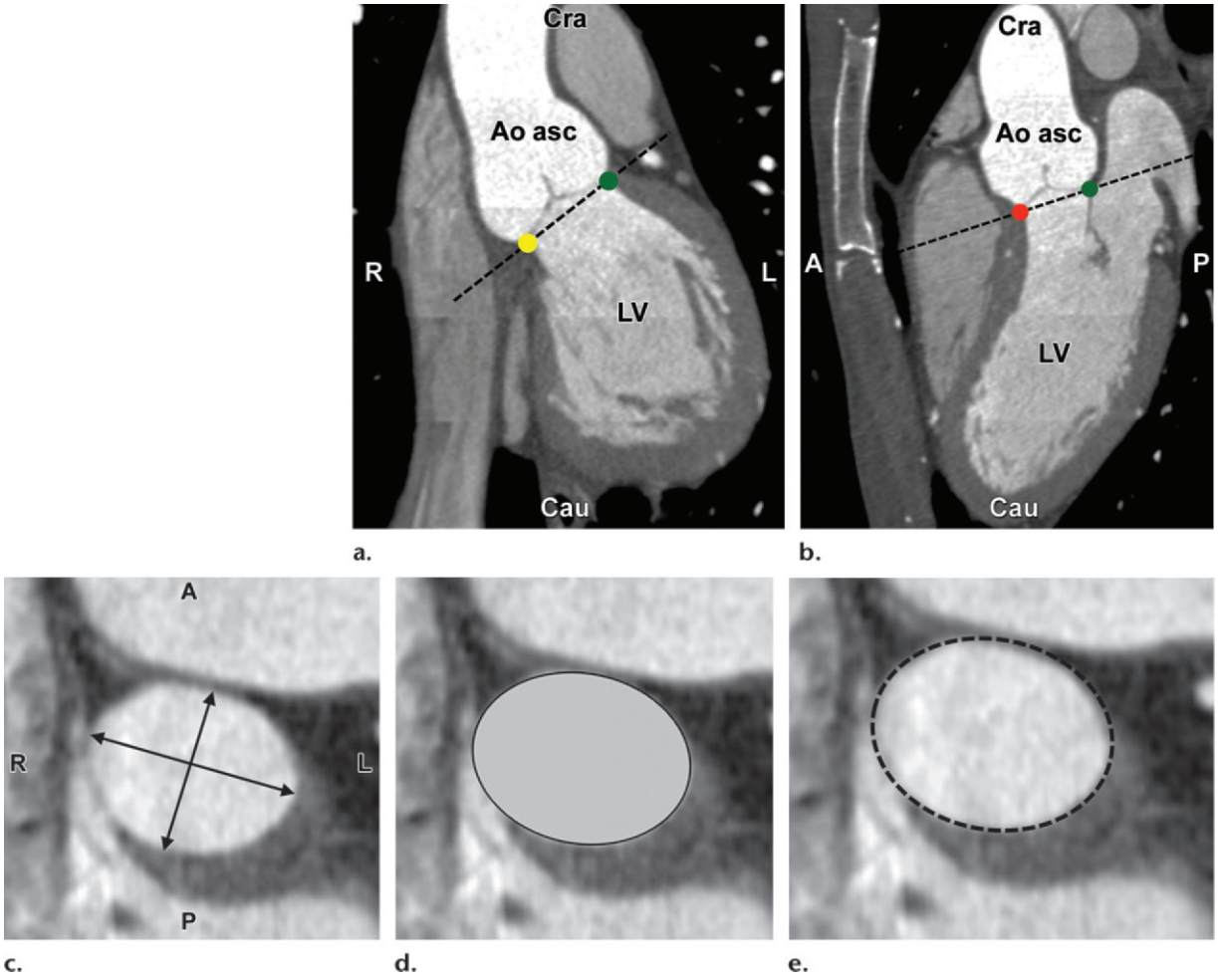

Figure 12. Possible measurements of the aortic annulus. Before taking any measurement, a correctly reformatted image along the annular plane must be obtained. This is achieved by interactively manipulating the reconstruction planes on a workstation so that the nadirs of all three cusps are identified on one transverse image. **(a, b)** Standard coronal **(a)** and sagittal **(b)** images are in themselves not suitable but can be used as a starting point, with the final double-oblique imaging plane (dashed line) containing the basal attachment points of the left coronary (green dot), right coronary (orange dot), and noncoronary (yellow dot) cusps. *A* = anterior, *Ao asc* = ascending aorta, *Cau* = caudal, *Cra* = cranial, *P* = posterior. **(c–e)** The resulting cross-sectional image can then be used to measure the true long- and short-axis annular diameters (arrows in **c**), the annular area (shaded oval in **d**), and the annular perimeter (dashed line in **e**). From each of these different types of measurements, the mean area diameter can be derived using the appropriate formula. *A* = anterior, *P* = posterior.

and shown to not only help reduce paravalvular regurgitation, but also the combined endpoint of in-hospital death, annular rupture, valve-in-valve implantation, and valve embolization (71).

For self-expandable valves, other authors have suggested perimeter-based multidetector CT sizing with a recommended oversizing of the annular circumference by approximately 10%–25% (68,72,73). This approach is probably more in keeping with the persistent annular eccentricity after deployment in this kind of valve.

Although these multidetector CT sizing proposals represent a thoughtful first step in more formal integration of multidetector CT in transcatheter valve selection, it is important to emphasize that, because Medtronic and Edwards Lifesciences valves have different properties (Table 1), the results of studies of one type of valve are not applicable across vendors. Furthermore, the value of echocardiography in the sizing process must not be underestimated, since available randomized trial data and the great majority of TAVR outcome data have been successfully based on (2D) TEE-derived measurements. Thus, valve size selection remains a multifactorial and multimodality process.

Finally, although 3D annular measurements obtained with multidetector CT have been shown to help predict PAR retrospectively (74), there is only limited prospective large-scale evidence that integrating multidetector CT in annular sizing and transcatheter valve selection will improve clinical outcomes (71).

Figure 13. Double-oblique contrast-enhanced CT image through the aortic sinus reveals extensive leaflet calcifications, most prominently in the right coronary cusp. Prominent valve calcification may complicate device deployment and may be associated with an increased risk for postoperative paravalvular regurgitation. *A* = anterior, *P* = posterior.

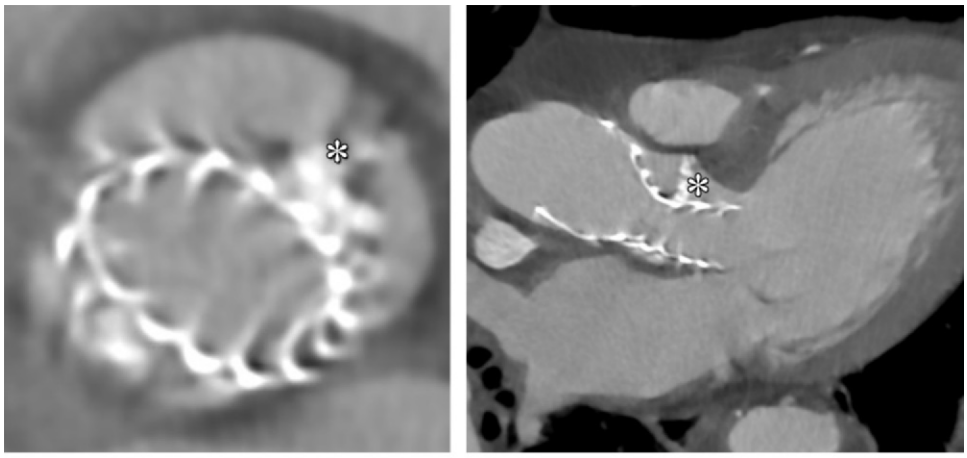

a. **b.**

Figure 14. Contrast-enhanced CT image at the level of the sinuses of Valsalva **(a)** and three-chamber view **(b)** show a CoreValve device in the aortic root. The obstructive effect of the extensive calcifications of the native aortic valve (*) causes asymmetric deployment and positioning of the transcatheter valve. Despite a very convincing finding of severe paravalvular regurgitation at CT, echocardiography revealed only moderate regurgitation, underscoring the need to compare results from different imaging modalities to achieve the most complete assessment possible.

Native Aortic Valve: Further Imaging Features and Relationship to the Coronary Artery Ostia

Multidetector CT has proved to be an excellent tool for the accurate assessment of the morphology of the aortic valve, with a recent study further indicating excellent correlation between the degree of valve calcification and the hemodynamic severity of aortic valve stenosis (75). TTE remains the primary tool for morphologic and functional evaluation of the aortic valve; in a recent study, however, CT proved superior in characterizing the morphology of the aortic valve, with better differentiation between bicuspid and tricuspid valves (76). This is important, since the procedure can be technically more challenging in bicuspid valves (77). There is increasing evidence that the presence, extent, and distribution of valve calcifications may have a role in the occurrence of peri- and postprocedural complications (61,78,79). Extensive valve calcification has been associated with moderate to significant valve regurgitation after TAVR (80–82), presumably due to interposition of these bulky calcifications between the deploying device and the native aortic valve (Figs 13, 14) (80). Furthermore, owing to the same proposed mechanism of restricted deployment, extensive calcifications at the sinotubular junction can limit balloon expansion, possible leading to inadequate device fixation and subsequent migration into the ascending aorta (83).

Displacement of the native aortic valve leaflets during deployment of the transcatheter valve carries a minimal but nevertheless important risk of subsequent occlusion of the coronary ostia, with a reported incidence of 0.6%–4.1% (28,84). Although this is typically a periprocedural complication, it has also been reported to occur hours after valve implantation (85). Increased awareness of this rare complication is required in patients with large and heavily calcified valve leaflets and a short anatomic distance from the annular plane to the ostia of the coronary arteries (Fig 15) (86). Furthermore, this distance has been shown to have significant interindividual variation ranging from 7.1 to 21.7 mm (45). As a general rule, a minimum distance of 10 mm between the annular plane and the coronary ostia is recommended (87). Finally, the size of the aortic sinus could also play a role in this complication, since this structure acts as a "reservoir" for displaced native aortic valves. However, there are no strict guidelines regarding a minimum required size for the aortic sinus that would preclude intervention. Preoperative risk evaluation is therefore based on an overall subjective assessment of *(a)* the amount and distribution of calcifications in the native aortic valve, and *(b)* the capacity of the aortic sinus to accommodate the displaced native valve after deployment.

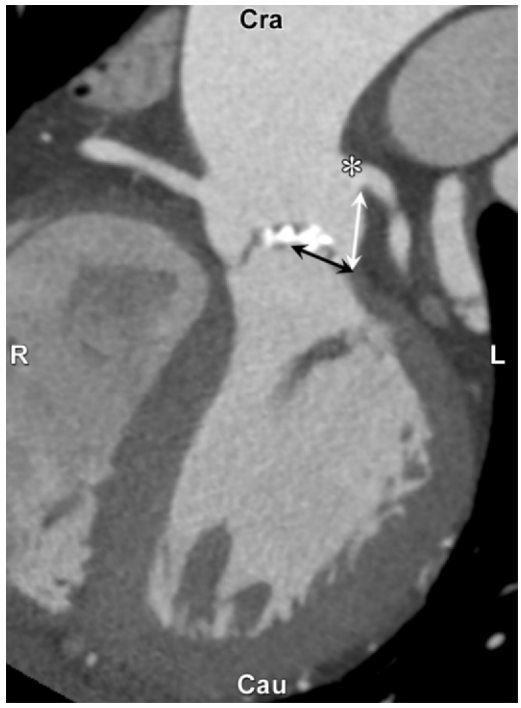

Figure 15. Slightly oblique coronal contrast-enhanced CT image at the level of the aortic root shows that an adequate distance (white double-headed arrow) between the annular plane and the nearest coronary ostium—in this case, the left main ostium (*)—is necessary to avoid the rare but devastating complication of ostial occlusion due to displaced native valve leaflets during prosthesis deployment. As a rule of thumb, a minimum distance of 10 mm is recommended. It is also recommended that this distance be greater than the length of the aortic valve leaflets (black double-headed arrow). *Cau* = caudal, *Cra* = cranial.

Determining the Best Fluoroscopic Projection Angle for Device Deployment

During the actual TAVR procedure, the 3D visualization offered by multidetector CT is reduced to the 2D projection image inherent in conventional angiography. Nevertheless, a correct periprocedural understanding on the part of the operator of the spatial orientation of the aortic root relative to the body axis is necessary to correctly position the prosthetic device along the centerline of the aortic root and perpendicular to the aortic annular plane. Without multidetector CT guidance, the operator needs to perform several intravenous contrast material injections to find the optimal fluoroscopic projection plane for deployment, with the nadirs of the three aortic valve cusps aligned in the same straight 2D projected plane (Fig 16). Besides adding complexity to the procedure, this step introduces an additional contrast volume load and increased risk for subsequent renal injury. Multidetector CT, with its excellent 3D capabilities, has been shown to help preoperatively predict a suitable angulation (left anterior oblique–right anterior oblique and cranial-caudal angles) of the angiography tube and achieve precise positioning of the prosthetic valve following angiography of the aortic root (88,89), thereby significantly improving the final transcatheter valve position compared with procedures performed without multidetector CT guidance (89). These tube angulation data can be obtained manually through manipulation of the multidetector CT dataset as explained by some authors (24,88), or derived using specialized software tools (90). In each individual case, there are several possible appropriate angles (24,90). At our institution, this information is routinely derived and consistently reported at each preoperative CT examination using software-derived measurements (Advantage Windows AW 4.3, GE Healthcare). However, the increasing availability of 3D rotational angiography systems also allows accurate assessment of the best projection plane, reducing the role of multidetector CT for this purpose (56).

Other Preprocedural Findings

Multidetector CT can help accurately evaluate the curvature of the ascending aorta and its anatomic relation to the left subclavian artery,

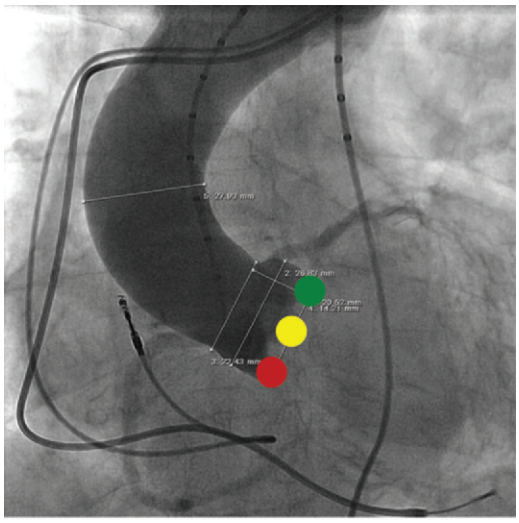

a.

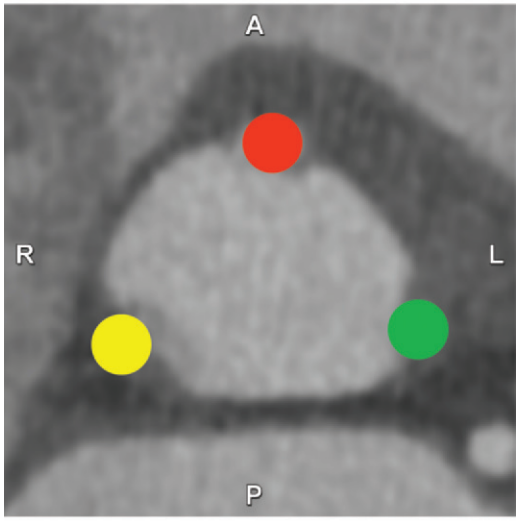

b.

Figure 16. For optimal device deployment, the inclination of the angiography tube must be such that, on the resulting fluoroscopic image **(a)**, the basal insertion sites of all aortic valve leaflets are aligned in the same anatomic annular plane, corresponding with the correctly aligned double-oblique CT image **(b)**. Green dot = left coronary cusp, orange dot = right coronary cusp, yellow dot = noncoronary cusp. On the basis of preprocedural CT-derived left anterior oblique–right anterior oblique and cranial-caudal angulation values, an accurate prediction of the best procedural fluoroscopic angulation for correct deployment of the transcatheter valve along an axis perpendicular to the aortic annular plane can be made. This approach obviates repeated angiographic test injections to determine the correct tube angulation, thereby reducing both the amount of contrast material used and the time required for the procedure. *A* = anterior, *P* = posterior.

since anatomic variations, increased angulation, and/or tortuosity of these vessels will increase the technical difficulty of the procedure. Likewise, augmented angulation between the ascending aorta and the aortic root–LVOT will complicate the accurate positioning of the transcatheter valve with endovascular access, since this angulation can induce some rotation of the transcatheter valve during deployment (although it is not a contraindication for the procedure) (Fig 17). Furthermore, the presence of a hypertrophic basal septum can theoretically undermine the stability of the transcatheter valve due to its mass effect during and after deployment (Fig 17b).

In transapical device deployment, the angle between the left ventricular apex and the aortic annular plane has been described as one of the determinants of success, since rigid delivery systems can make the procedure more difficult at steeper angles (91).

Although the aforementioned anatomic characteristics are not considered strict procedural contraindications, they are valuable for preoperative strategy evaluation and must always be included in the radiology report. Nevertheless, there are as yet no strict guidelines, with the final assessment being left to the performing surgeon and interventional cardiologist.

Incidental Findings

Because the investigated subgroup of TAVR candidates are invariably advanced in age, the presence of significant incidental findings that may alter the treatment course must always be considered. Therefore, with its large anatomic coverage, multidetector CT is an ideal screening tool, in one series helping detect significant incidental disease in up to 34.3% of cases and unsuspected malignancy in 4.1% (34). However, untreated symptomatic aortic valve stenosis has a dismal prognosis, with short-term survival rates even

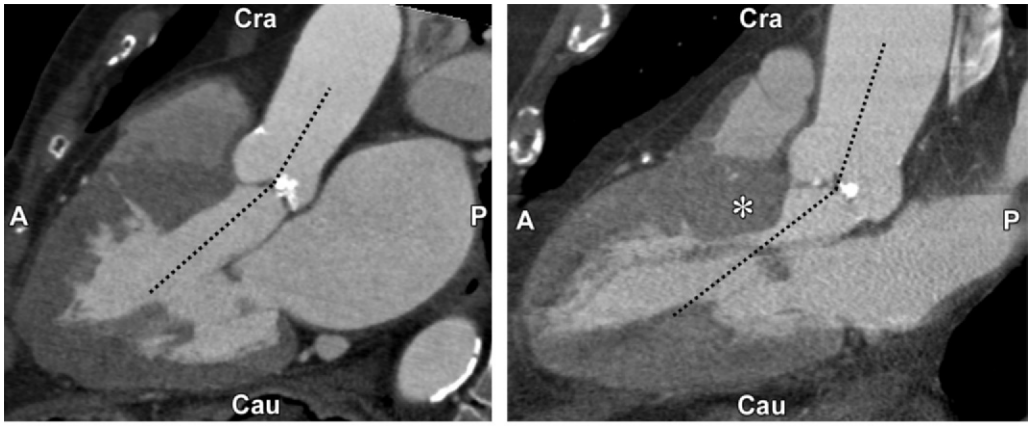

a. b.

Figure 17. CT evaluation of the angulation between the ascending aorta, aortic root, and LVOT. A practically straight line between the ascending aorta and the LVOT (dashed line in **a)** indicates a much more favorable anatomic situation than does a steeper angulation (dashed line in **b)**, since the latter can complicate stable deployment of the prosthesis. The technical difficulty of the procedure is further increased by the presence of a hypertrophic basal septum (* in **b**), potentially creating increased resistance during device deployment. *A* = anterior, *Cau* = caudal, *Cra* = cranial, *P* = posterior.

lower than those of some undetected malignancies. Therefore, treatment options must always be reviewed on a case-by-case basis.

Postprocedural Imaging

The exact role of multidetector CT in the postprocedural evaluation of patients who have undergone transcatheter valve implantation remains unclear. Although the role of multidetector CT in the detection of periaortic complications (eg, pseudoaneurysms) is unquestioned, its purpose in helping evaluate causes of valve dysfunction is currently the subject of debate and intense investigation. CT can be used to evaluate the position and expansion of the transcatheter valve in the aortic root (Fig 14); however, it is not yet known which morphologic parameters can help in the assessment of paravalvular regurgitation. This further underscores the need to compare results obtained with different imaging modalities to achieve the most complete evaluation possible.

Conclusion

Given the favorable outcomes described in this article and the increasing age of the Western population, it is not surprising that there is increasing worldwide interest in the application and further development of TAVR procedures. The development of a transcatheter-based alternative for aortic valve replacement has rapidly gained favor in the treatment of symptomatic aortic valve stenosis in the nonsurgical patient cohort. The roles of different noninvasive imaging techniques, especially multidetector CT, have been discussed in detail, along with the specific advantages and limitations of each technique. Finally, it must be borne in mind that annular sizing and valve selection is a multifactorial and multidisciplinary process in which all available clinical and imaging data must be included to achieve the most complete assessment possible.

***Disclosures of Conflicts of Interest.*—J.A.L.:** *Activities related to the present article:* consultant for Edwards Lifesciences. *Activities not related to the present article:* consultant for GE Healthcare, speakers bureau for Edwards Lifesciences and GE Healthcare. *Other relationships:* disclosed no relevant relationships.

References

1. Baumgartner H, Hung J, Bermejo J, et al. Echocardiographic assessment of valve stenosis: EAE/ASE recommendations for clinical practice. J Am Soc Echocardiogr 2009;22(1):1–23.
2. Rosamond W, Flegal K, Furie K, et al. Heart disease and stroke statistics: 2008 update—a report from the American Heart Association Statistics Committee and Stroke Statistics Subcommittee. Circulation 2008;117(4):e25–e146.
3. Nkomo VT, Gardin JM, Skelton TN, Gottdiener JS, Scott CG, Enriquez-Sarano M. Burden of valvular heart diseases: a population-based study. Lancet 2006;368(9540):1005–1011.
4. Iung B, Baron G, Butchart EG, et al. A prospective survey of patients with valvular heart disease in Europe: the Euro Heart Survey on Valvular Heart Disease. Eur Heart J 2003;24(13):1231–1243.
5. Freeman RV, Otto CM. Spectrum of calcific aortic valve disease: pathogenesis, disease progression, and treatment strategies. Circulation 2005;111(24):3316–3326.
6. Hammermeister KE, Sethi GK, Henderson WG, Oprian C, Kim T, Rahimtoola S. A comparison

of outcomes in men 11 years after heart-valve replacement with a mechanical valve or bioprosthesis. Veterans Affairs Cooperative Study on Valvular Heart Disease. N Engl J Med 1993;328(18): 1289–1296.
7. Horstkotte D, Loogen F. The natural history of aortic valve stenosis. Eur Heart J 1988;9(suppl E):57–64.
8. Bose AK, Aitchison JD, Dark JH. Aortic valve replacement in octogenarians. J Cardiothorac Surg 2007;2:33.
9. Bakaeen FG, Chu D, Huh J, Carabello BA. Is an age of 80 years or greater an important predictor of short-term outcomes of isolated aortic valve replacement in veterans? Ann Thorac Surg 2010;90 (3):769–774.
10. Florath I, Albert A, Boening A, Ennker IC, Ennker J. Aortic valve replacement in octogenarians: identification of high-risk patients. Eur J Cardiothorac Surg 2010;37(6):1304–1310.
11. Smith CR, Leon MB, Mack MJ, et al. Transcatheter versus surgical aortic-valve replacement in high-risk patients. N Engl J Med 2011;364(23):2187–2198.
12. Leon MB, Smith CR, Mack M, et al. Transcatheter aortic-valve implantation for aortic stenosis in patients who cannot undergo surgery. N Engl J Med 2010;363 (17):1597–1607.
13. Ussia GP, Barbanti M, Petronio AS, et al. Transcatheter aortic valve implantation: 3-year outcomes of self-expanding CoreValve prosthesis. Eur Heart J 2012;33(8):969–976.
14. Bosmans JM, Kefer J, De Bruyne B, et al. Procedural, 30-day and one year outcome following CoreValve or Edwards transcatheter aortic valve implantation: results of the Belgian National Registry. Interact Cardiovasc Thorac Surg 2011;12(5):762–767.
15. Coeytaux RR, Williams JW Jr, Gray RN, Wang A. Percutaneous heart valve replacement for aortic stenosis: state of the evidence. Ann Intern Med 2010; 153(5):314–324.
16. Kodali SK, Williams MR, Smith CR, et al. Two-year outcomes after transcatheter or surgical aortic-valve replacement. N Engl J Med 2012;366(18): 1686–1695.
17. Makkar RR, Fontana GP, Jilaihawi H, et al. Transcatheter aortic-valve replacement for inoperable severe aortic stenosis. N Engl J Med 2012;366(18): 1696–1704.
18. Bauernschmitt R, Schreiber C, Bleiziffer S, et al. Transcatheter aortic valve implantation through the ascending aorta: an alternative option for no-access patients. Heart Surg Forum 2009;12(1):E63–E64.
19. Bruschi G, De Marco F, Fratto P, et al. Direct aortic access through right minithoracotomy for implantation of self-expanding aortic bioprosthetic valves. J Thorac Cardiovasc Surg 2010;140 (3):715–717.
20. Stortecky S, Buellesfeld L, Wenaweser P, Windecker S. Transcatheter aortic valve implantation: the procedure. Heart 2012;98(suppl 4):iv44–iv51.
21. Philipsen TE, Rodrigus IE, Claeys MJ, Bosmans JM. Alternative access in transcatheter aortic valve implantation: brachiocephalic artery access. Innovations (Phila) 2012;7(5):372–375.
22. Ye J, Cheung A, Lichtenstein SV, et al. Transapical aortic valve implantation in humans. J Thorac Cardiovasc Surg 2006;131(5):1194–1196.
23. Grube E, Laborde JC, Gerckens U, et al. Percutaneous implantation of the CoreValve self-expanding valve prosthesis in high-risk patients with aortic valve disease: the Siegburg first-in-man study. Circulation 2006;114(15):1616–1624.
24. Leipsic J, Hague CJ, Gurvitch R, Ajlan AM, Labounty TM, Min JK. MDCT to guide transcatheter aortic valve replacement and mitral valve repair. Cardiol Clin 2012;30(1):147–160.
25. Webb JG, Altwegg L, Masson JB, Al Bugami S, Al Ali A, Boone RA. A new transcatheter aortic valve and percutaneous valve delivery system. J Am Coll Cardiol 2009;53(20):1855–1858.
26. Fraccaro C, Napodano M, Tarantini G, et al. Expanding the eligibility for transcatheter aortic valve implantation: the trans-subclavian retrograde approach using the III generation CoreValve revalving system. JACC Cardiovasc Interv 2009;2(9):828–833.
27. Nietlispach F, Wijesinghe N, Wood D, Carere RG, Webb JG. Current balloon-expandable transcatheter heart valve and delivery systems. Catheter Cardiovasc Interv 2010;75(2):295–300.
28. Thomas M, Schymik G, Walther T, et al. Thirty-day results of the SAPIEN aortic Bioprosthesis European Outcome (SOURCE) Registry: a European registry of transcatheter aortic valve implantation using the Edwards SAPIEN valve. Circulation 2010; 122(1):62–69.
29. Tchetche D, Dumonteil N, Sauguet A, et al. Thirty-day outcome and vascular complications after transarterial aortic valve implantation using both Edwards Sapien and Medtronic CoreValve bioprostheses in a mixed population. EuroIntervention 2010;5(6):659–665.
30. Van Mieghem NM, Nuis RJ, Piazza N, et al. Vascular complications with transcatheter aortic valve implantation using the 18 Fr Medtronic CoreValve system: the Rotterdam experience. EuroIntervention 2010;5 (6):673–679.
31. Leon MB, Piazza N, Nikolsky E, et al. Standardized endpoint definitions for transcatheter aortic valve implantation clinical trials: a consensus report from the Valve Academic Research Consortium. Eur Heart J 2011;32(2):205–217.
32. Toggweiler S, Gurvitch R, Leipsic J, et al. Percutaneous aortic valve replacement: vascular outcomes with a fully percutaneous procedure. J Am Coll Cardiol 2012;59(2):113–118.
33. Kurra V, Schoenhagen P, Roselli EE, et al. Prevalence of significant peripheral artery disease in patients evaluated for percutaneous aortic valve insertion: preprocedural assessment with multidetector computed tomography. J Thorac Cardiovasc Surg 2009;137(5): 1258–1264.
34. Ben-Dor I, Waksman R, Hanna NN, et al. Utility of radiologic review for noncardiac findings on multislice computed tomography in patients with severe aortic stenosis evaluated for transcatheter aortic valve implantation. Am J Cardiol 2010;105(10):1461–1464.
35. Hayashida K, Lefèvre T, Chevalier B, et al. Transfemoral aortic valve implantation new criteria to predict vascular complications. JACC Cardiovasc Interv 2011;4(8):851–858.
36. Achenbach S, Delgado V, Hausleiter J, Schoenhagen P, Min JK, Leipsic JA. SCCT expert consensus document on computed tomography imaging before transcatheter aortic valve implantation (TAVI)/transcatheter aortic valve replacement (TAVR). J Cardiovasc Comput Tomogr 2012;6(6):366–380.
37. Masson JB, Kovac J, Schuler G, et al. Transcatheter aortic valve implantation: review of the nature, management, and avoidance of procedural complications. JACC Cardiovasc Interv 2009;2(9):811–820.
38. Vahanian A, Alfieri O, Al-Attar N, et al. Transcatheter valve implantation for patients with aortic

stenosis: a position statement from the European Association of Cardio-Thoracic Surgery (EACTS) and the European Society of Cardiology (ESC), in collaboration with the European Association of Percutaneous Cardiovascular Interventions (EAPCI). EuroIntervention 2008;4(2):193–199.
39. Blanke P, Euringer W, Baumann T, et al. Combined assessment of aortic root anatomy and aortoiliac vasculature with dual-source CT as a screening tool in patients evaluated for transcatheter aortic valve implantation. AJR Am J Roentgenol 2010;195(4): 872–881.
40. Wuest W, Anders K, Schuhbaeck A, et al. Dual source multidetector CT-angiography before transcatheter aortic valve implantation (TAVI) using a high-pitch spiral acquisition mode. Eur Radiol 2012; 22(1):51–58.
41. Plank F, Friedrich G, Bartel T, et al. Benefits of high-pitch 128-slice dual-source computed tomography for planning of transcatheter aortic valve implantation. Ann Thorac Surg 2012;94(6):1961–1966.
42. Schueller-Weidekamm C, Schaefer-Prokop CM, Weber M, Herold CJ, Prokop M. CT angiography of pulmonary arteries to detect pulmonary embolism: improvement of vascular enhancement with low kilovoltage settings. Radiology 2006;241 (3):899–907.
43. Hur J, Kim YJ, Lee HJ, et al. Dual-enhanced cardiac CT for detection of left atrial appendage thrombus in patients with stroke: a prospective comparison study with transesophageal echocardiography. Stroke 2011;42(9):2471–2477.
44. de Heer LM, Budde RP, Mali WP, de Vos AM, van Herwerden LA, Kluin J. Aortic root dimension changes during systole and diastole: evaluation with ECG-gated multidetector row computed tomography. Int J Cardiovasc Imaging 2011;27(8): 1195–1204.
45. Tops LF, Wood DA, Delgado V, et al. Noninvasive evaluation of the aortic root with multislice computed tomography implications for transcatheter aortic valve replacement. JACC Cardiovasc Imaging 2008;1(3):321–330.
46. Shiran A, Adawi S, Ganaeem M, Asmer E. Accuracy and reproducibility of left ventricular outflow tract diameter measurement using transthoracic when compared with transesophageal echocardiography in systole and diastole. Eur J Echocardiogr 2009; 10(2):319–324.
47. Bertaso AG, Wong DT, Liew GY, et al. Aortic annulus dimension assessment by computed tomography for transcatheter aortic valve implantation: differences between systole and diastole. Int J Cardiovasc Imaging 2012;28(8):2091–2098.
48. Hamdan A, Guetta V, Konen E, et al. Deformation dynamics and mechanical properties of the aortic annulus by 4-dimensional computed tomography: insights into the functional anatomy of the aortic valve complex and implications for transcatheter aortic valve therapy. J Am Coll Cardiol 2012;59(2): 119–127.
49. Anderson RH. Clinical anatomy of the aortic root. Heart 2000;84(6):670–673.
50. Piazza N, de Jaegere P, Schultz C, Becker AE, Serruys PW, Anderson RH. Anatomy of the aortic valvar complex and its implications for transcatheter implantation of the aortic valve. Circ Cardiovasc Interv 2008;1(1):74–81.
51. Anderson RH. Demystifying the anatomic arrangement of the aortic valve. Eur J Cardiothorac Surg 2006;29(6):1006–1007.
52. Dashkevich A, Blanke P, Siepe M, et al. Preoperative assessment of aortic annulus dimensions: comparison of noninvasive and intraoperative measurement. Ann Thorac Surg 2011;91(3): 709–714.
53. Smíd M, Ferda J, Baxa J, et al. Aortic annulus and ascending aorta: comparison of preoperative and perioperative measurement in patients with aortic stenosis. Eur J Radiol 2010;74(1):152–155.
54. Al Ali AM, Altwegg L, Horlick EM, et al. Prevention and management of transcatheter balloon-expandable aortic valve malposition. Catheter Cardiovasc Interv 2008;72(4):573–578.
55. Altiok E, Koos R, Schröder J, et al. Comparison of two-dimensional and three-dimensional imaging techniques for measurement of aortic annulus diameters before transcatheter aortic valve implantation. Heart 2011;97(19):1578–1584.
56. Meyhöer J, Ahrens J, Neuss M, Hölschermann F, Schau T, Butter C. Rotational angiography for preinterventional imaging in transcatheter aortic valve implantation. Catheter Cardiovasc Interv 2012;79 (5):756–765.
57. La Manna A, Sanfilippo A, Capodanno D, et al. Cardiovascular magnetic resonance for the assessment of patients undergoing transcatheter aortic valve implantation: a pilot study. J Cardiovasc Magn Reson 2011; 13:82.
58. Paelinck BP, Van Herck PL, Rodrigus I, et al. Comparison of magnetic resonance imaging of aortic valve stenosis and aortic root to multimodality imaging for selection of transcatheter aortic valve implantation candidates. Am J Cardiol 2011;108(1):92–98.
59. Burman ED, Keegan J, Kilner PJ. Aortic root measurement by cardiovascular magnetic resonance: specification of planes and lines of measurement and corresponding normal values. Circ Cardiovasc Imaging 2008;1(2):104–113.
60. Jabbour A, Ismail TF, Vazir A, et al. Multimodality imaging in transcatheter aortic valve implantation: comparison between cardiovascular magnetic resonance, cardiac computed tomography, transesophageal and transthoracic echocardiography. J Cardiovasc Magn Reson 2012;14(suppl 1):P98.
61. Delgado V, Ng AC, van de Veire NR, et al. Transcatheter aortic valve implantation: role of multi-detector row computed tomography to evaluate prosthesis positioning and deployment in relation to valve function. Eur Heart J 2010;31(9):1114–1123.
62. Messika-Zeitoun D, Serfaty JM, Brochet E, et al. Multimodal assessment of the aortic annulus diameter: implications for transcatheter aortic valve implantation. J Am Coll Cardiol 2010;55(3):186–194.
63. Tamburino C, Capodanno D, Ramondo A, et al. Incidence and predictors of early and late mortality after transcatheter aortic valve implantation in 663 patients with severe aortic stenosis. Circulation 2011;123(3):299–308.
64. Détaint D, Lepage L, Himbert D, et al. Determinants of significant paravalvular regurgitation after transcatheter aortic valve: implantation impact of device and annulus discongruence. JACC Cardiovasc Interv 2009;2(9):821–827.
65. Takagi K, Latib A, Al-Lamee R, et al. Predictors of moderate-to-severe paravalvular aortic regurgitation immediately after CoreValve implantation and the impact of postdilatation. Catheter Cardiovasc Interv 2011;78(3):432–443.
66. Sherif MA, Abdel-Wahab M, Stöcker B, et al. Anatomic and procedural predictors of paravalvular aortic regurgitation after implantation of the

Medtronic CoreValve bioprosthesis. J Am Coll Cardiol 2010;56(20): 1623–1629.
67. Gurvitch R, Webb JG, Yuan R, et al. Aortic annulus diameter determination by multidetector computed tomography: reproducibility, applicability, and implications for transcatheter aortic valve implantation. JACC Cardiovasc Interv 2011;4(11): 1235–1245.
68. Schultz CJ, Moelker A, Piazza N, et al. Three dimensional evaluation of the aortic annulus using multislice computer tomography: are manufacturer's guidelines for sizing for percutaneous aortic valve replacement helpful? Eur Heart J 2010;31(7):849–856.
69. Tzikas A, Schultz CJ, Piazza N, et al. Assessment of the aortic annulus by multislice computed tomography, contrast aortography, and trans-thoracic echocardiography in patients referred for transcatheter aortic valve implantation. Catheter Cardiovasc Interv 2011;77(6):868–875.
70. Willson AB, Webb JG, Freeman M, et al. Computed tomography-based sizing recommendations for transcatheter aortic valve replacement with balloon-expandable valves: comparison with transesophageal echocardiography and rationale for implementation in a prospective trial. J Cardiovasc Comput Tomogr 2012;6(6):406–414.
71. Binder R, Webb JG, Urena M, Hansson N. The impact of integration of a computed tomography annulus area sizing algorithm on clinical outcomes of transcatheter aortic valve replacement: a prospective, multicenter, controlled trial. J Am Coll Cardiol 2013 May 15. [Epub ahead of print]
72. Piazza N, Lange R. Imaging of valvular heart disease: I can see clearly now—anatomy of the aortic valve. http://org.crsti.dliv2010.s3.amazonaws.com/pdfs/034_Ovality_of_the_aortic_valve_ annulus.pdf. Accessed April 30, 2013.
73. Schultz CJ, Weustink A, Piazza N, et al. Geometry and degree of apposition of the CoreValve revalving system with multislice computed tomography after implantation in patients with aortic stenosis. J Am Coll Cardiol 2009;54(10):911–918.
74. Willson AB, Webb JG, Labounty TM, et al. 3-dimensional aortic annular assessment by multidetector computed tomography predicts moderate or severe paravalvular regurgitation after transcatheter aortic valve replacement: a multicenter retrospective analysis. J Am Coll Cardiol 2012; 59(14):1287–1294.
75. Cueff C, Serfaty JM, Cimadevilla C, et al. Measurement of aortic valve calcification using multislice computed tomography: correlation with haemodynamic severity of aortic stenosis and clinical implication for patients with low ejection fraction. Heart 2011; 97(9):721–726.
76. Tanaka R, Yoshioka K, Niinuma H, Ohsawa S, Okabayashi H, Ehara S. Diagnostic value of cardiac CT in the evaluation of bicuspid aortic stenosis: comparison with echocardiography and operative findings. AJR Am J Roentgenol 2010;195(4):895–899.
77. Wijesinghe N, Ye J, Rodés-Cabau J, et al. Transcatheter aortic valve implantation in patients with bicuspid aortic valve stenosis. JACC Cardiovasc Interv 2010;3(11):1122–1125.
78. Koos R, Mahnken AH, Dohmen G, et al. Association of aortic valve calcification severity with the degree of aortic regurgitation after transcatheter aortic valve implantation. Int J Cardiol 2011;150(2):142–145.
79. John D, Buellesfeld L, Yuecel S, et al. Correlation of device landing zone calcification and acute procedural success in patients undergoing transcatheter aortic valve implantations with the self-expanding CoreValve prosthesis. JACC Cardiovasc Interv 2010;3(2):233–243.
80. Zegdi R, Ciobotaru V, Noghin M, et al. Is it reasonable to treat all calcified stenotic aortic valves with a valved stent? results from a human anatomic study in adults. J Am Coll Cardiol 2008;51(5):579–584.
81. Haensig M, Lehmkuhl L, Rastan AJ, et al. Aortic valve calcium scoring is a predictor of significant paravalvular aortic insufficiency in transapical-aortic valve implantation. Eur J Cardiothorac Surg 2012;41(6):1234–1240; discussion 1240–1241.
82. Marwan M, Achenbach S, Ensminger SM, et al. CT predictors of post-procedural aortic regurgitation in patients referred for transcatheter aortic valve implantation: an analysis of 105 patients. Int J Cardiovasc Imaging 2013;29(5):1191–1198.
83. Kapadia SR, Schoenhagen P, Stewart W, Tuzcu EM. Imaging for transcatheter valve procedures. Curr Probl Cardiol 2010;35(5):228–276.
84. Stabile E, Sorropago G, Cioppa A, et al. Acute left main obstructions following TAVI. EuroIntervention 2010;6(1):100–105.
85. Spiro J, Nadeem A, Doshi SN. Delayed left main stem obstruction following successful TAVI with an Edwards SAPIEN XT valve: successful resuscitation and percutaneous coronary intervention using a non-invasive automated chest compression device (AutoPulse). J Invasive Cardiol 2012; 24(5):224–228.
86. Webb JG, Chandavimol M, Thompson CR, et al. Percutaneous aortic valve implantation retrograde from the femoral artery. Circulation 2006;113(6):842–850.
87. Delgado V, Ewe SH, Ng AC, et al. Multimodality imaging in transcatheter aortic valve implantation: key steps to assess procedural feasibility. EuroIntervention 2010;6(5):643–652.
88. Kurra V, Kapadia SR, Tuzcu EM, et al. Pre-procedural imaging of aortic root orientation and dimensions: comparison between x-ray angiographic planar imaging and 3-dimensional multidetector row computed tomography. JACC Cardiovasc Interv 2010;3(1):105–113.
89. Gurvitch R, Wood DA, Leipsic J, et al. Multislice computed tomography for prediction of optimal angiographic deployment projections during transcatheter aortic valve implantation. JACC Cardiovasc Interv 2010;3(11):1157–1165.
90. Tzikas A, Schultz C, Van Mieghem NM, de Jaegere PP, Serruys PW. Optimal projection estimation for transcatheter aortic valve implantation based on contrast-aortography: validation of a prototype software. Catheter Cardiovasc Interv 2010;76(4):602–607.
91. Falk V, Walther T, Schwammenthal E, et al. Transapical aortic valve implantation with a self-expanding anatomically oriented valve. Eur Heart J 2011;32(7):878–887.

Preprocedural CT Evaluation of Transcatheter Aortic Valve Replacement: What the Radiologist Needs to Know

Rodrigo A. Salgado, MD • Jonathon A. Leipsic, MD • Bharati Shivalkar, MD, PhD • Lenz Ardies, MD • Paul L. Van Herck, MD, PhD • Bart J. Op de Beeck, MD • Christiaan Vrints, MD, PhD • Inez Rodrigus, MD, PhD • Paul M. Parizel, MD, PhD • Johan Bosmans, MD, PhD

RadioGraphics 2014; 34:1491–1514 • **Published online** 10.1148/rg.346125076 • **Content Codes:** CA CH CT

Page 1492
Several studies have identified various subgroups of patients with a substantially elevated risk for surgery-related complications or death, with some series reporting inoperability in up to 32% of cases. Factors contributing to a substantially increased surgical risk include frailty and old age, prior radiation therapy with significant chest damage, a heavily calcified aorta, severe pulmonary or hepatic disease, and chest deformities. Surgical risk is also increased in the presence of depressed renal function, previous stroke, peripheral vascular disease, and reduced left ventricular function. Because untreated symptomatic aortic valve stenosis has a dismal short-term prognosis, a less rigorous approach is needed for this subgroup of patients.

Page 1493
Basically, a TAVR procedure consists of deploying a bioprosthetic aortic valve in the aortic root after transporting the device from a chosen entry point.

Page 1493
With the current commercially available devices, TAVR is technically possible when the aortic annular diameter is between 18 and 29 mm (range for the two devices combined).

Pages 1494–1495
Both device- and anatomy-related obstacles may alter the chosen access pathway or even make the procedure impossible to perform via the endovascular pathway regardless of device-compatible aortic root dimensions. Therefore, multidetector CT plays an important role in examining the potential access routes and reporting any possible problems that may alter the chosen access strategy

Page 1501
[T]here are currently no universally validated strict guidelines regarding the exact use of multidetector CT or any other 3D imaging tool for patient selection and device sizing across all platforms. Therefore, it is important to realize that in practice, the process of clinical patient evaluation, annular sizing, and evaluation of access route for final transcatheter heart valve selection and placement is multifactorial, integrating both clinical data and information from all available imaging modalities.